Nat. Hazards Earth Syst. Sci., 26, 3637–3665, 2026
https://doi.org/10.5194/nhess-26-3637-2026

Natural Hazards and Earth System Sciences
Open Access

Dynamic spatial modelling of mass movement impacts for large areas: a data-driven framework for impact-based early warning

Stefan Steger[1], **Raphael Spiekermann**[1], **Mateo Moreno**[2], **Sebastian Lehner**[1,3], **Katharina Enigl**[1,3], **Alice Crespi**[4], and **Matthias Schlögl**[1,5]

[1]GeoSphere Austria, Vienna, Austria
[2]OpenGeoHub Foundation, Doorwerth, the Netherlands
[3]Department for Meteorology and Geophysics, University of Vienna, Vienna, Austria
[4]Center for Climate Change and Transformation, Eurac Research, Bozen/Bolzano, Italy
[5]Department of Landscape, Water and Infrastructure, BOKU University, Vienna, Austria

Correspondence: Stefan Steger (stefan.steger@geosphere.at)

Received: 6 October 2025 – Discussion started: 15 October 2025
Revised: 22 June 2026 – Accepted: 24 July 2026 – Published: 6 August 2026

Abstract. Early warning systems play a crucial role in mitigating the impacts of severe weather events and related hazards. Traditional systems typically focus on meteorological forecasts and often do not account for the potential consequences that may follow, unlike impact-based approaches. In densely populated mountainous regions, such as the Alps, heavy precipitation frequently causes damaging mass movements. Since mass movement impacts ultimately result from a complex interplay of meteorological, geo-environmental, and socio-economic factors, warnings based solely on precipitation may have limited effectiveness. This study introduces a flexible, dynamic, and spatially explicit modelling framework for supporting impact-based early warning of precipitation-induced mass movement processes. The framework is tailored to three movement types: slides, flows, and falls. It integrates predisposing, preparatory, and triggering conditions, combining geo-environmental, meteorological, and exposure data to estimate daily impact potential for an Alpine core study area covering more than 91 000 km^2 (Austria and South Tyrol), and subsequently explores the transferability of these relationships to the wider Alpine region, subject to important limitations. Using Generalized Additive Mixed Models (GAMMs), the approach captures nonlinear relationships between impacts and predictors, ensuring interpretability and operational relevance. Further key elements include incorporation of potential runout paths while maintaining a basin-based landscape representation, focusing model training on relevant terrain and time-periods to avoid trivial predictions, generating interpretable outputs, and illustrating potential applicability through time-series predictive maps derived from hindcasting and "what-if" scenarios. Results indicate promising performance of slide- and flow-type models for the core study area, suggesting potential for operational application, while the fall-type model shows limited applicability for early warning, likely due to its lower sensitivity to short-term weather conditions. The primary contribution of this research lies in demonstrating a transferable and generalizable modelling framework, rather than delivering an operational regional warning system. Beyond early warning, the framework shows broad applicability for analysing spatio-temporal patterns, conducting trend analyses, and assessing climate change impacts. This research advances the fields of landslide prediction and impact-based warning by providing a transferable and generalizable approach, offering actionable insights for disaster risk reduction and climate adaptation strategies.

1 Introduction

Early warning systems play an important role in reducing the impacts of severe weather events and associated hazards. Traditionally, these systems have been focused on meteorological forecasts over large areas, predicting critical meteorological conditions such as strong winds, hail or heavy precipitation (Alfieri et al., 2012; Sun et al., 2014; Weyrich et al., 2018; Sivle et al., 2022). While effective in identifying potentially hazardous weather conditions in advance, traditional warnings do not explicitly address the negative consequences that may follow. To improve risk management and promote more appropriate responses, it is essential to assess how critical weather conditions may impact lives, livelihoods, and property (WMO, 2015; Casteel, 2016; Weyrich et al., 2020). Accordingly, several national meteorological and hydrological services now aim to account for the potential impacts of weather phenomena to better inform decision-makers and the public (Uccellini and Hoeve, 2019; Kaltenberger et al., 2020; Potter et al., 2021; Sivle et al., 2022).

Impact-oriented approaches primarily rely on meteorological information, emphasizing expected weather conditions while using expert judgment to infer potential impacts. In contrast, impact-based approaches offer a more quantitative assessment of potential consequences by explicitly integrating meteorological data with geo-environmental and socio-economic data, including exposure and vulnerability (Kaltenberger et al., 2020; Potter et al., 2021). The transition toward impact-based warnings is encouraged by the World Meteorological Organization and international frameworks, such as the Sendai Framework for Disaster Risk Reduction and the United Nations Early Warnings for All initiative, which advocate for integrated, risk-informed strategies (WMO, 2015). Approaches for deriving impact-based warnings have been demonstrated for various phenomena, such as hailstorms, windstorms, droughts and flood-related assessments (Merz et al., 2020; Alfieri et al., 2024; Najafi et al., 2024; Schmid et al., 2024; Oh and Bartos, 2025). However, to our knowledge, no operational examples currently exist where impact potential is spatially modelled at high temporal resolution for hillslope processes, such as mass movements across large areas.

Even the step preceding impact-based forecasting, namely predicting the geomorphic phenomenon itself, remains a major challenge. Several examples of operational or prototypal landslide warning systems exist in the Alpine region, including examples from Italy, Switzerland, and Slovenia (Auflič et al., 2016; Wicki et al., 2020; Tiranti and Ronchi, 2023; Segoni et al., 2025), as well as in other countries such as Norway (Krøgli et al., 2018). However, even where operational systems exist, they are generally considered complex and uncertain, while their underlying modelling framework mainly focuses on process prediction, not impact (Alfieri et al., 2012; Piciullo et al., 2018; Guzzetti et al., 2020). The complexity stems from the underlying intricate interplay between meteorological conditions and geo-environmental drivers, which is difficult to capture using available data over large areas. Their occurrence involves processes operating across different timescales, from static predisposing conditions to dynamic preparatory factors and short-term triggers (Crozier, 1989). For instance, slide-type movements are influenced by static factors, including slope morphology and subsurface material type, while preparatory factors, like antecedent rainfall or seasonal vegetation changes, can affect how a hillslope reacts to external triggers, such as intense precipitation (Luna and Korup, 2022; Steger et al., 2023). Other mass movement types, like flow-type or fall-type movements, may be driven by distinct causal factors and therefore require tailored modelling approaches (Loche et al., 2022). Differentiating between movement types and their respective drivers is often overlooked in large-area assessments or, when acknowledged, remains difficult to address due to resource and data limitations (Günther et al., 2014; Caleca et al., 2025).

A further challenge lies in assessing landslide impacts, as triggered landslides travel downslope and can damage assets located far from their release zones. Consequently, spatially explicit landslide runout models are essential for impact and risk evaluations (Horton et al., 2013; Mergili et al., 2015; Wichmann, 2017). However, many spatially explicit large-area landslide assessments focus primarily on release zones or do not distinguish between release areas and downslope movement paths. This limitation reduces the ability of conventional landslide susceptibility models to evaluate impacts within the potential reach of landslides, such as flat terrain at the base of hillslopes (Mergili et al., 2019; Lima et al., 2023; Marchesini et al., 2024).

Beyond the widespread use of static landslide susceptibility models that indicate where landslides may occur (Reichenbach et al., 2018) and empirical rainfall thresholds that focus on critical precipitation conditions for their initiation (Brunetti et al., 2010; Segoni et al., 2018; Peres and Cancelliere, 2021; Kaitna et al., 2025), recent efforts have increasingly focused on data-driven space-time landslide modelling (Lombardo et al., 2020). These models dynamically estimate critical landslide conditions across space and time by integrating geo-environmental factors with dynamic conditions, most notably weather-related variables (Stanley et al., 2021; Maraun et al., 2022; Ahmed et al., 2023; Moreno et al., 2024; Nocentini et al., 2024; Mondini et al., 2025). Most of these approaches focus on critical conditions within landslide release zones, without explicitly accounting for downslope landslide propagation or the assets located in potentially affected areas. Thus, despite being dynamic and spatially explicit, they lack key components essential for impact-based warning, such as information on elements at risk, which are explicitly addressed in landslide risk or exposure assessments (Dai et al., 2002; Corominas et al., 2013; Lin et al., 2023; Marchesini et al., 2024; Caleca et al., 2025). So far, landslide risk or exposure assessments for large areas only occasionally incorporate dynamic factors, such as land cover changes or climate trends (Farvacque et al., 2019; Ozturk et al., 2022; Lin et al., 2023). However, their utility for early warning is limited, as they fail to capture short-term meteorological variability and therefore cannot provide predictions at daily or sub-daily scales.

From a technical viewpoint, flexible algorithms and software tools offer extensive capabilities for processing large and heterogeneous datasets to create space-time models over large areas. However, their effectiveness in assessing and predicting environmental hazards and risks often remains limited by the quality and completeness of the input data used to train these models (Ardizzone et al., 2002; Guzzetti et al., 2006; Reichenbach et al., 2018). In fact, data limitations are frequently identified as a key barrier to more detailed large-area landslide modelling (Günther et al., 2014; Broeckx et al., 2018; Caleca et al., 2025). For instance, data-driven landslide models often have limited explanatory power due to spatially incomplete and temporally inconsistent landslide training data, which can lead to biased results. Targeted sampling and modelling strategies are required to adequately address these challenges or, at the very least, careful model interpretation (Steger et al., 2021; Caleca et al., 2025; Luna et al., 2025). Avoiding a high raster resolution or using alternative landscape representations, such as slope units or basins, can help reduce the impact of inaccuracies in landslide inventories on modelling results (Alvioli et al., 2016; Woodard et al., 2024). However, such generalizations can obscure important details. For instance, in landslide risk or exposure assessments, infrastructure or populations located within a mapping unit but well beyond the actual reach of potential landslides may be erroneously counted as exposed, simply because the entire unit is considered susceptible (Caleca et al., 2025).

The sampling strategy used to represent typical landslide and non-landslide conditions strongly influences subsequent modelling results (Guo et al., 2024). Including data from irrelevant trivial terrain or trivial time periods, such as flat areas or dry conditions, can lead to landslide models that learn and reproduce overly simplistic patterns while inflating model performance scores. For example, such apparently well-performing models may mainly separate steep from flat areas or rainy from dry days, missing conditions critical for decision-making (Steger and Glade, 2017; Steger et al., 2023).

Model interpretability becomes particularly important when outputs are used to support decision-making (Schlögl et al., 2025b), especially in early warning contexts (Vinuesa and Sirmacek, 2021; Reichstein et al., 2025). Transparent and interpretable outputs facilitate effective communication with stakeholders and foster trust in model results (Schlögl et al., 2025a). For modellers, interpretable outputs are equally valuable, as they support plausibility checks and iterative refinements throughout the development process (Lombardo et al., 2020; Collini et al., 2022; Nocentini et al., 2023; Caleca et al., 2024).

In summary, many large-area landslide assessments remain of limited use for impact-based warning purposes. This is often due to their static nature, which fails to capture short-term meteorological variability, their exclusive focus on initiation zones while overlooking downslope runout areas and exposed assets, and limitations related to data availability and modelling design. This study addresses these gaps by developing and evaluating interpretable, data-driven models to dynamically assess the daily impact potential of precipitation-induced mass movement processes for a large area covering Austria and South Tyrol (91 000 km^2), while treating non-validated spatial extrapolation to the wider Alpine region (450 000 km^2) as a demonstrator to explore the potential applicability of the framework to very large terrain. The models are designed to assess the impact potential of three movement types, namely slides, flows and falls, on infrastructure.

Key features of the proposed approach include:

- Integration of impact drivers: Capturing the interplay of meteorological, geo-environmental and exposure data by integrating predisposing, preparatory and triggering conditions.
- Incorporation of runout paths: Accounting for movement paths while maintaining a generalized landscape representation by incorporating pixel-based mass movement runout information into basin-based model training.
- Tailored sampling strategies: Avoiding oversimplified patterns by constraining model training to non-trivial terrain and time-periods.
- Model interpretability: Generating explainable outputs that support process-oriented plausibility checks and effective communication of results.
- Illustrating potential suitability for impact-based warning: Producing maps and animations for hindcasting and scenario-based examples.

The modelling framework presented in this study is designed as a generalizable and transferable approach for dynamically estimating the impact potential of fast-onset hazards within an impact-based warning context.

2 Study area

This study focuses on an Alpine core study area covering Austria and the Italian province of South Tyrol (91 000 km^2), which forms the basis for model development and model evaluation. The broader Alpine Space, as delineated by the Interreg Alpine Space Programme of the European Union, encompasses approximately 450 000 km^2 across seven countries (Austria, France, Germany, Italy, Liechtenstein, Slovenia, and Switzerland) and is considered for demonstrator-based spatial extrapolation (Fig. 1).

The Alpine Space represents a distinctive and heterogeneous mountainous system within Europe, encompassing high alpine terrain, peri-alpine lowlands and densely populated valleys. Elevations range from sea level in the southern coastal areas to elevations of more than 4800 m above sea level in the Western European Alps (Fig. 1). The considerable elevation gradient along the Alpine arc results in high

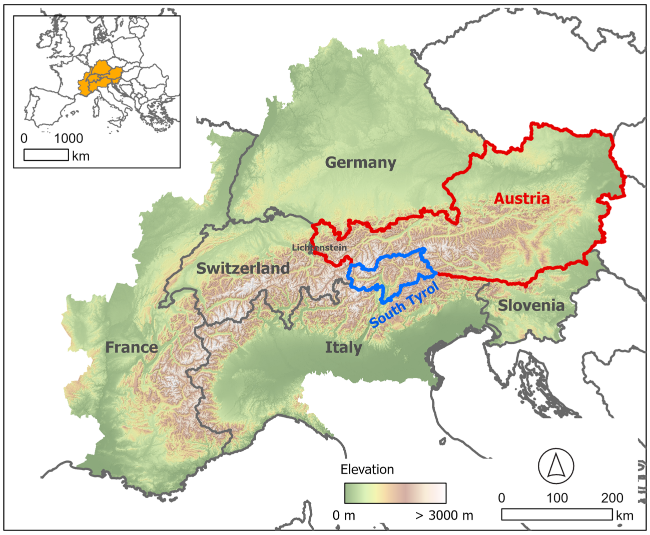

Figure 1. Location and topography of the study area. Austria (red) and South Tyrol (blue) indicate the core study area for model training and quantitative validation, while the wider Alpine Space represents the domain used for spatial extrapolation.

relief energy, which plays a key role in conditioning slope instability.

The hillslope basins in the Alpine Space are lithologically diverse (Donnini et al., 2020). Sandstone and claystone formations represent the dominant class within approximately 34 % of the basins used in this study, followed by mixed carbonate rocks making up 28 % and pure carbonate rocks approximately 23 %. Igneous rocks, both acid and mafic types, cover 10 %, while metamorphic rocks account for approximately 5 %. This lithological diversity reflects the complex geological context of the region and plays a significant role in shaping soil development, hydrological processes and slope stability (Donnini et al., 2020; Sidle and Ochiai, 2006).

Land cover also plays an important role in mass movement occurrence through various hydrological and mechanical effects (Crozier, 1989). Land cover data shows that the study area includes a considerable proportion of forested land, with broadleaf and coniferous tree cover accounting for approximately 38 % of the area (Malinowski et al., 2020). Agricultural lands, including cultivated areas and vineyards, account for approximately 23 %, while grasslands and shrub-dominated areas, including herbaceous vegetation, sclerophyllous cover and moorlands, comprise around 27 %. Artificial surfaces, including urban infrastructure, represent a relatively small portion at 4 %. Wetlands, bare natural surfaces, permanent snow-covered areas and water bodies together contribute around 8 % (Malinowski et al., 2020).

A range of climate-related factors contribute to mass movement occurrence, with precipitation and temperature being the most influential, while snowmelt, seasonal variability and specific weather types also play important roles (Gariano and Guzzetti, 2016). Climatically, the region exhibits a high degree of variability in both temperature and precipitation. Temperature variations are pronounced due to the complex topography between valleys, ridges and mountain tops, as well as diverse climatic influences. These include maritime influences from the Atlantic Ocean and Mediterranean Sea, and continental effects from Eastern Europe. Precipitation is shaped mainly by the prevailing meandering westerly wind belt, moisture sources from the Atlantic and Mediterranean, and characteristic pathways of low-pressure systems. In addition, seasonal variations and local orographic effects also contribute to precipitation dynamics (Schär et al., 1998; Hofstätter and Chimani, 2012; Ménégoz et al., 2020).

Across the Alps, various elements at risk are exposed, including population, infrastructure, cultural heritage and critical assets (Alfieri et al., 2012; Günther et al., 2014; Keiler and Fuchs, 2016; Caleca et al., 2025). From a socio-economic perspective, the Alpine Space is home to over 80 million people and includes both major European metropolitan centres and remote rural regions. The area contains densely populated transport corridors, particularly within narrow valley systems where natural hazard-prone terrain overlaps with human settlements, leading to elevated exposure levels. Thus, development in the Alpine region is intrinsically coupled with natural hazard risk, with landslides representing an important component (Fuchs et al., 2017; Schlögl et al., 2019). A visual overview of geo-environmental variables (e.g., topography, land cover, lithology), mean annual precipitation, and exposure-related features (e.g., buildings, roads) across the Alpine Space can be explored through the basin-based dataset provided in the repository.

3 Data

Topographic information was sourced from a 20 m Digital Terrain Model (DTM) covering the entirety of Europe (Sonny, 2023; Fig. 1). The DTM served as the foundation for delineating basins, for mapping potential landslide process paths and for deriving morphometric predictor variables. Lithological data was derived from the Alpine Geo-Lithological Map (Alpine-Geo-LiM) developed by Donnini et al. (2020). This map offers a simplified and harmonized lithological classification of the Alpine arc at a scale of 1 : 1 000 000 and was derived from national geological maps of Austria, France, Germany, Italy, Slovenia and Switzerland. Information on land cover was obtained from the Pan-European land cover and land use map published by Malinowski et al. (2020). The dataset provides consistent land cover information for the year 2017 across Europe and is based on an automated classification of multi-temporal Sentinel-2 imagery. Meteorological data for the period 2005 to 2020 were obtained from the Copernicus European Regional ReAnalysis (CERRA), which provides high-resolution (5.5 km) gridded climate data for Europe. Temperature variables were derived from CERRA, while precipitation variables were taken from its Land component (CERRA-Land) (Ridal et al., 2024). Temperature was available at 3 hourly temporal resolution from CERRA analysed fields. These were aggregated to daily minimum/mean/maximum fields and then reprojected to EPSG:32632. Precipitation data from CERRA-Land are available directly as daily analysed fields, hence no further preprocessing except for the reprojection was needed. This dataset has already demonstrated promising potential for linking meteorological conditions to landslide occurrence in the Alps (Crespi et al., 2026). Exposure data was sourced from building and infrastructure layers available in OpenStreetMap (OSM), a widely used source of volunteered geographic information that provides comprehensive and regularly updated cartographic data, with the highest data completeness observed in Europe (Goodchild, 2007; Zhou et al., 2022).

Model training and quantitative validation were conducted within the core Alpine study area covering Austria and the Italian province of South Tyrol (Fig. 4), while predictor datasets were created for the entire Alpine Space, technically enabling spatial extrapolation beyond the training domain. The training area comprises 3696 basins (Figs. 1, 4) and, in addition to time-stamped impact data, encompasses substantial diversity in geology, topography, land cover, and climatic features. The Alpine-wide generalization of input variables, including the reclassification of lithology and land cover (cf. Sect. 4.2.3), introduces inherent limitations and constrains the ability of the model to estimate impact potential beyond the training domain (cf. Sect. 6, Discussion).

Mass movement data were compiled from national inventories and filtered to include only precipitation-induced events (2005–2020) with known dates and documented infrastructure damage, ensuring relevance for impact-based analysis. Sources include the national GEORIOS inventory from GeoSphere Austria (Themessl et al., 2022), which provides time-stamped records of slides, flows and falls across Austria. From the event inventory of the Austrian Torrent and Avalanche Control (WLK), only flow-type events were extracted (BMNT, 2018; Heiser et al., 2019). The landslide data for South Tyrol, including slides, flows, and falls, originate from the provincial implementation of the national landslide inventory IFFI (Inventario dei Fenomeni Franosi in Italia), which contains explicit attributes on recorded impacts. IFFI data are generally accessible via the IdroGeo platform (Iadanza et al., 2021). While these inventories are subject to known limitations, they offer a valuable and comprehensive source of time-stamped mass movement occurrences enriched with contextual attributes. A notable characteristic, particularly limiting for purely process-oriented studies, is their tendency to underrepresent slope instabilities that did not cause damage (Trigila et al., 2010; Heiser et al., 2019; Steger et al., 2021). However, this focus on damage-causing events aligns well with the objectives of this study, which specifically targets an impact-based perspective.

4 Methods

4.1 Methodical framework

This research developed three daily-scale impact-based models, each specifically tailored to slide-, flow- and fall-type mass movements. Figure 2 presents the methodological framework of this study, with further details provided in Sect. 4.2 to 4.4.

In summary, the Alpine Space area was divided into 17 872 basins. Within each basin, areas potentially affected by a mass movement, hereafter referred to as potential process areas (PPAs), were delineated for each movement type to identify terrain where impacts are possible (Sect. 4.2.1). Movement type-specific binary response variables, representing presence and absence of impacts, were then generated using a spatio-temporal sampling scheme that restricts observations to relevant basins and relevant periods (Sect. 4.2.2). Predictor variables representing geo-environmental and exposure characteristics were aggregated within the PPAs of each basin, while daily meteorological data was aggregated to the basins using areal weighting (Sect. 4.2.3). Mass movement impacts were then modelled separately for each movement type as a function of meteorological, geo-environmental and exposure factors (Sect. 4.3). The data-driven models were evaluated using quantitative metrics and plausibility checks and then spatially transferred across the entire Alpine domain to generate daily impact predictions, visualized as maps and animations (Sect. 4.4).

4.2 Data preparation

4.2.1 Basin Delineation and Mapping of Potential Process Area

The Alpine Space was first subdivided into 17 872 hydrological half-basins using the r.watershed module in GRASS GIS 8.4 based on a resampled 50 m DTM (Neteler et al., 2012). Throughout the paper, these spatial units are referred to as basins. The basins have a median size of 2020 ha, with a lower threshold of 200 ha (Figs. 3, 4). Polygons smaller than 200 ha were successively merged with adjacent units, first prioritizing the longest shared boundary, and subsequently the largest neighbouring area. Then, PPAs were delineated separately for each movement type to account for areas where mass movement impacts can reasonably be expected (Fig. 3a, b). This step was essential to focus the analysis within each basin on non-trivial terrain, thereby excluding irrelevant features beyond the potential reach of mass movements. Given the Alpine-wide scale, the Gravitational Process Path (GPP) model (Wichmann, 2017) was used to identify potential runout paths based on the available 20 m DTM. Our approach combined the angle of reach concept with stochastic random walk routing along the surface of a DTM, balancing realism and computational efficiency to ap-

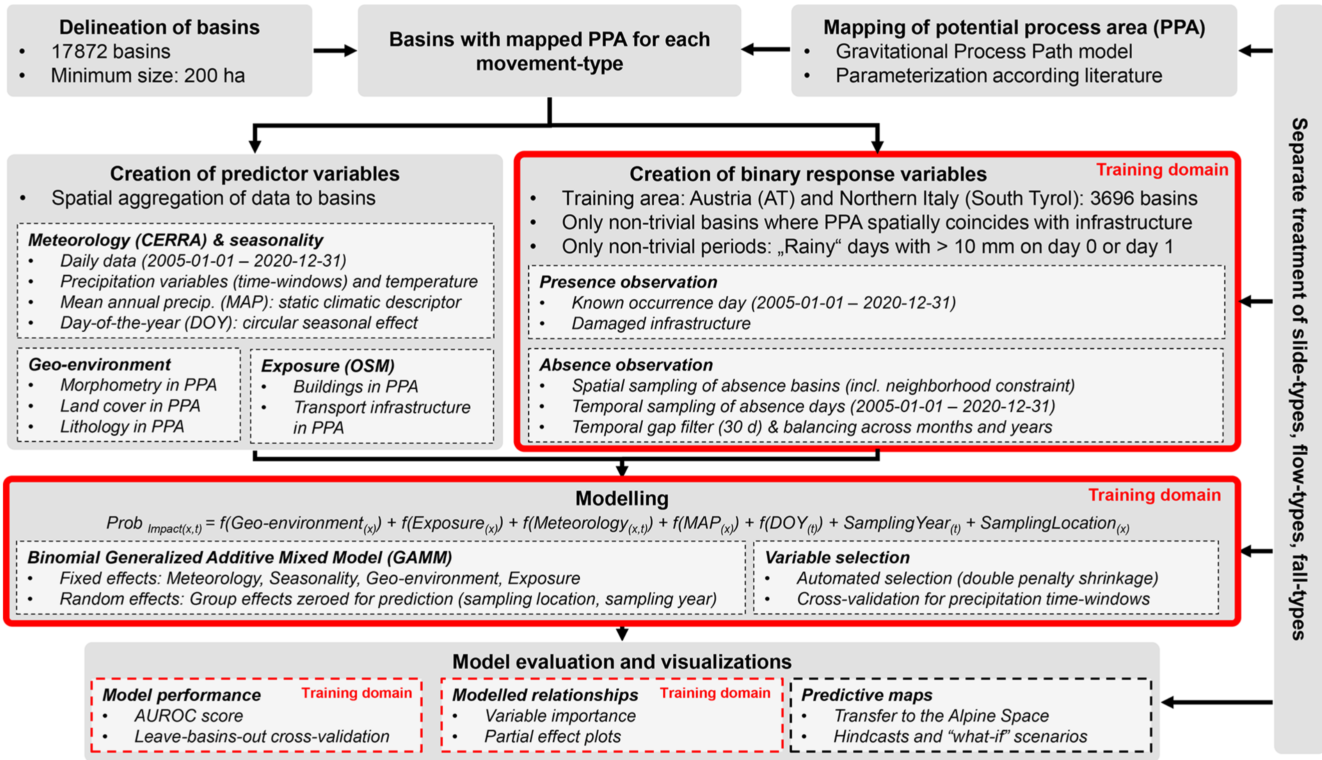

Figure 2. Methodical framework of this study. Aspects referring exclusively to the training domain (Austria, South Tyrol) are highlighted in red, while processing steps applied to the entire Alpine Space are shown without red borders.

proximate areas potentially affected by mass movements. Although less precise than site-specific runout models, the derived PPAs were considered to serve as meaningful spatial constraints for further analyses.

Parameterization for each movement type was derived from literature and the GPP model documentation (Wichmann, 2017). The GPP model first requires spatially explicit information on potential release areas to serve as starting points for subsequent process path simulations. The potential release areas were defined based on literature using conservative slope thresholds selected to capture a broad extent of likely initiation-prone terrain. From each potential release pixel, five random walks were initiated to capture some variability in downslope routing. For slide-types, slopes between 5 and 50° were considered potential release locations (Steger et al., 2021). Flow-type release areas were delineated on terrain with slopes greater than 15° (Horton et al., 2013), while fall-type release areas were mapped on slopes exceeding 35° (Dupire et al., 2020).

The angle of reach is an empirical parameter that primarily governs the resulting runout length, while runout behaviour was controlled by three parameters: slope weighting, divergence exponent and the persistence factor (Wichmann, 2017). For slide-type movements, an angle of reach of 22° was applied (D'Amboise et al., 2021), with a slope weighting of 30, a divergence exponent of 2.12 and a persistence value of 1.75 (Wichmann, 2017). Flow-type movements used an angle of reach of 11° (Horton et al., 2013), with the same slope weighting, divergence exponent and persistence values as slide-types. For fall-type movements, an angle of reach of 29° was used (Menk et al., 2023), combined with a slope weighting of 60, a divergence exponent of 1.75 and a persistence of 1.3 (Wichmann, 2017).

4.2.2 Response variables: Representing occurrence and non-occurrence of mass movement impact

For each movement type, a binary response variable representing the presence and absence of mass movement impact was created using a structured spatio-temporal sampling scheme within the core study area covering Austria and South Tyrol (Fig. 4). All observations, presences and absences, were limited to "non-trivial" situations. Spatially, only basins where infrastructure overlapped with the PPA were considered and temporally, only days with at least moderate precipitation were included. Thus, subsequent modelling was constrained to observations representing conditions potentially relevant for impact-based warning.

In detail, presence data were prepared using three data sources, GEORIOS, WLK and IFFI (Sect. 3, Fig. 4). Initially, all records of deep-seated movements or those lacking documented infrastructure impact were excluded, based on avail-

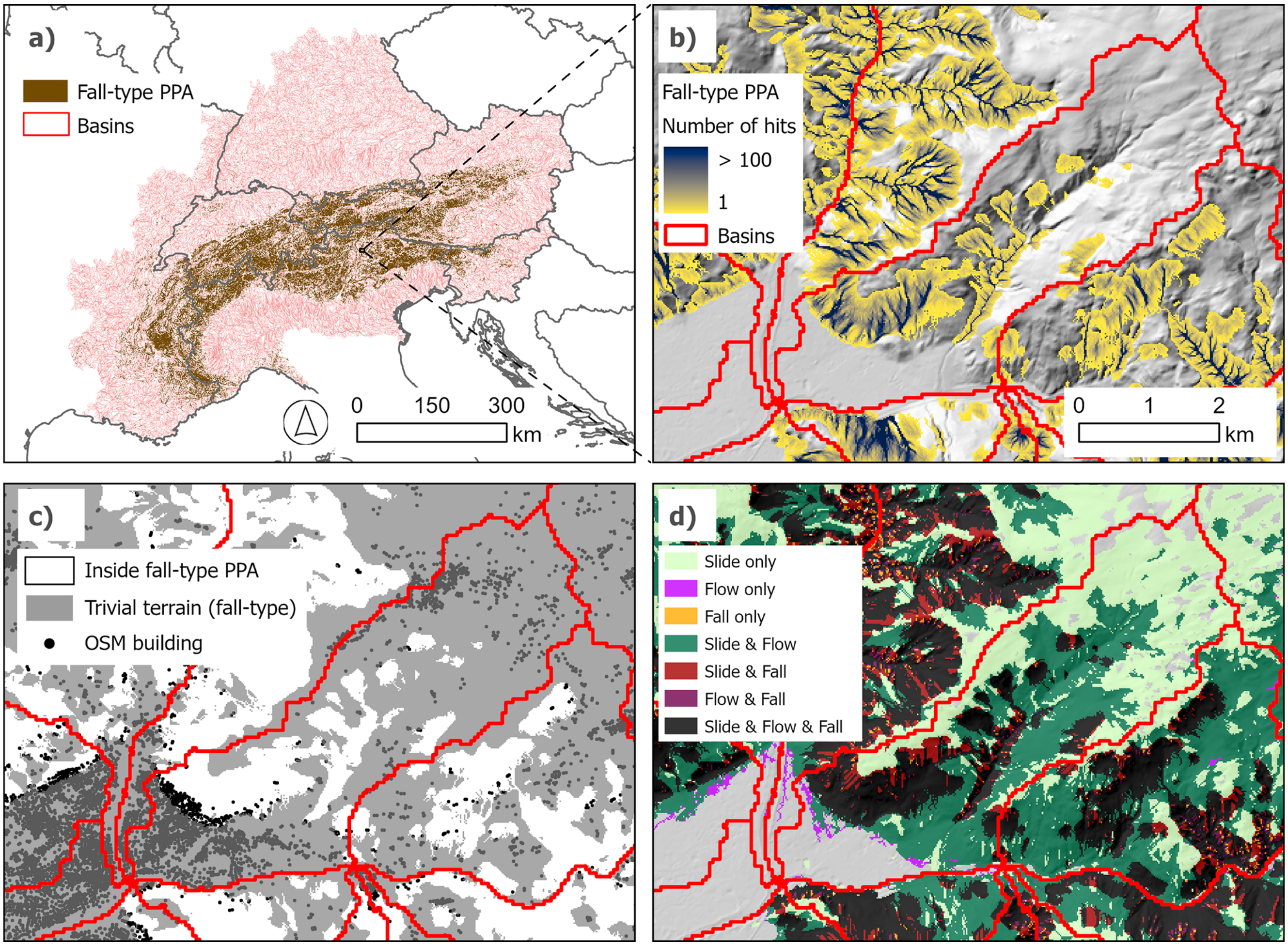

Figure 3. Basins and potential process areas (PPA) for fall-type movements across the Alpine Space **(a)**. Close-up of Bozen/Bolzano in South Tyrol, showing process paths for fall-types that were used to delineate the PPA **(b)**. Trivial terrain for fall-types, the PPA for fall-types and OSM building data **(c)**. Note that geo-environmental and exposure variables were aggregated to the basins based on their distribution within the PPAs (white areas in **c**). Overview of all PPAs within the example basin **(d)**.

able inventory attributes. The remaining presence data were grouped into slide-, flow- and fall-type movements and spatially joined to their corresponding basins. Further filtering was applied to retain only events with a known day of occurrence between 2005 and 2020 that were associated with at least moderate precipitation conditions. Building on our previous work (i.e., Steger et al., 2023), a rainfall filter was applied using precipitation data from the event day and the preceding day. The inclusion of the preceding day was important to account for cases where e.g., rainfall occurred in the late evening, resulting in a mass movement that was initiated/recorded on the following day. An arbitrary threshold of 10 mm for daily precipitation was used to define a day with moderate precipitation amounts, applied to either day.

Absence basins were randomly selected using a spatial distance constraint to minimize the selection of neighbouring basins and reduce spatial autocorrelation. Specifically, if basins had centroids within 10 km of each other, only one basin was selected. This was done while maintaining a one-to-one ratio between presence and absence basins for each movement type, which resulted in 2028 basins for the slide-type (1014 presences and 1014 absences), 1382 basins for the flow-type (691 each) and 1098 basin for the fall-type (549 each).

Absence dates were sampled from both absence and presence basins. For each basin, 50 random dates between 2005 and 2020 were initially drawn, creating a large pool of absence days. To reduce potential temporal autocorrelation, absence dates within the same basin were excluded if they fell within 30 d of any registered mass movement event. Additionally, if multiple absence dates within the same basin were less than 30 d apart, only one date was retained. Based on this, further downsampling was applied to distribute absence dates evenly across months and years, ensuring equal representation of all time periods, in analogy to Steger et al. (2023). From this pool of evenly distributed and temporally

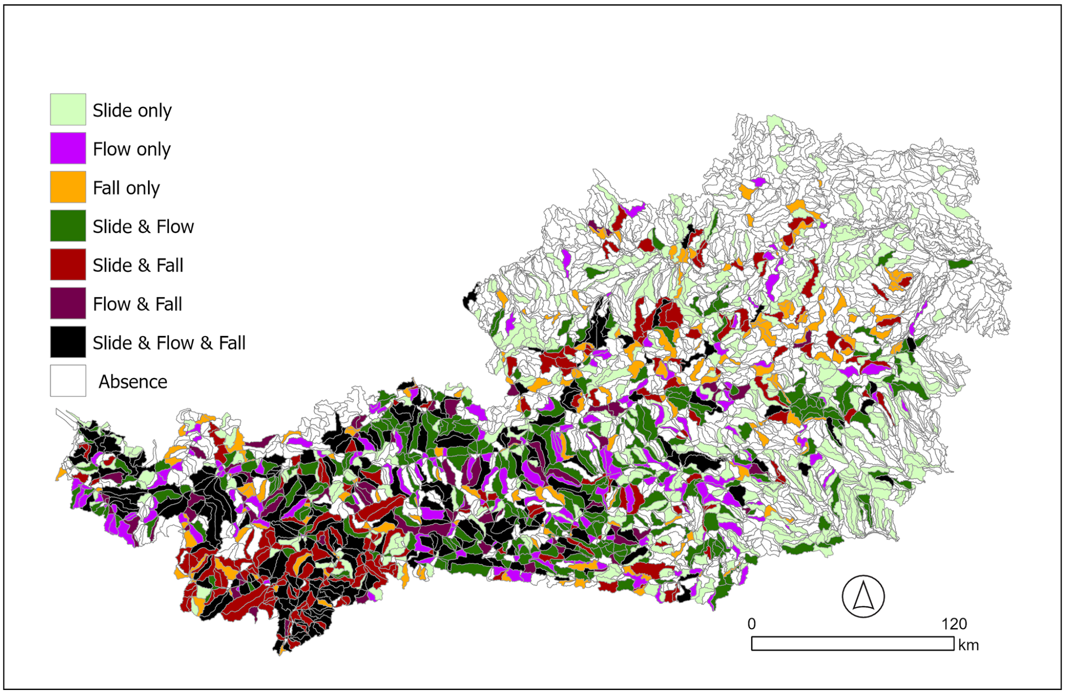

Figure 4. Map of the training area showing presence locations for each landslide movement type. Basins with slide-type presence observations comprise 1014 spatial units, flow-type 691 basins, and fall-type 549 basins. Note that the number of presence basins is lower than the total number of presence observations used for modelling, since multiple days with registered mass movement occurrences may have been recorded within a basin during the 16-year period.

spaced absence dates, only days meeting the same rainfall threshold as the presence data were retained to create a sample of at least moderately rainy days not associated with recorded mass movement occurrences. In summary, the final datasets comprised 7900 observations for the slide-type models (2077 presences and 5823 absences), 5463 observations for flow-type models (1386 presences and 4077 absences) and 4069 observations for fall-type models (647 presences and 3422 absences).

4.2.3 Predictor variables: Characterizing potential drivers of mass movement impact

A range of predictor variables was compiled for the entire Alpine Space to represent the geo-environmental, exposure-related and meteorological/climatic conditions. The following table shows the variables used to describe these conditions, along with their classification, spatial aggregation methods and spatio-temporal characteristics.

The static geo-environmental variables related to basin morphology were derived using SAGA GIS (Conrad et al., 2015) and the 20 m DTM. These variables were aggregated from the pixel level to the basin scale based on the respective PPAs. As a result, parameters, such as mean slope angle or the number of potentially exposed buildings, vary within the same basin, depending on the underlying movement type.

Land cover and lithology variables were based on reclassified versions of their original datasets (Donnini et al., 2020; Malinowski et al., 2020). The reduction in the number of classes aimed to increase the likelihood of obtaining interpretable and parsimonious models. Care was taken to ensure that each class was well represented within the training area, while also ensuring that no class occurring outside the training area lacked adequate representation in the training data. The four major land cover classes and five lithological classes are well represented within the training area and broadly distributed across the entire Alpine Space (Table 1).

Variables representing exposure were obtained from OSM and include buildings and transportation infrastructure. For buildings, individual point data were aggregated for each basin by summing the number of buildings within each PPA (Fig. 3c), resulting in approximately 19.8 million buildings within slide-type PPAs, 12.7 million in flow-type PPAs and 1.2 million in fall-type PPAs. Primary and secondary road networks and railways (e.g., highways, railways and paved roads) represented transport infrastructure, while trails and hiking paths were excluded. These data were aggregated for each basin by calculating the fraction of rasterised roads (20 m grid cells) within each PPA.

Temperature and precipitation fields at 5.5 km resolution were aggregated to the basin level using spatial weights based on the degree of overlap between CERRA grid cells

Table 1. Overview of predictor variables used for mass movement impact modelling, including their classification, spatial aggregation methods and spatio-temporal characteristics. Note that the variables in bold were included as candidates within the initial model setup (cf. Sect. 4.3).

Category	Variable (v) / Variable class (c)	Spatial aggregation	Type
Geo-environmental (Morphometry)	**Slope angle (v)**	Mean in PPA	Spatial and static
	Convergence (v)	Mean in PPA	
	Aspect (v)	Mean in PPA	
Geo-environmental (Land cover)	**Land cover (v)**	Dominant class in PPA	Spatial and static
	Deciduous forest (c)	Portion of class in PPA	
	Coniferous forest (c)	Portion of class in PPA	
	Crop- and grassland (c)	Portion of class in PPA	
	Bare surface and other (c)	Portion of class in PPA	
Geo-environmental (Lithology)	**Lithology (v)**	Dominant class in PPA	Spatial and static
	Igneous (c)	Portion of class in PPA	
	Metamorphic (c)	Portion of class in PPA	
	Mixed carbonate (c)	Portion of class in PPA	
	Pure carbonate (c)	Portion of class in PPA	
	Sandstone–claystone (c)	Portion of class in PPA	
Exposure	**Number of buildings (v)**	Number of buildings in PPA	Spatial and static
	Transport infrastructure (v)	Portion of "road" cells in PPA	
Meteorological (Precipitation)	**Short-term precipitation (v)**	Area-weighted spatial averaging	Spatial and daily
	Antecedent precipitation: 7, 14, 21, **30 d precipitation** (v)		
	Mean annual precipitation 2005–2020 (v)		Spatial and static
Meteorological (Temperature)	**Mean daily temperature (v)**	Area-weighted spatial averaging	Spatial and daily
	Binary: Day crossing 0 °C (v)		
	Binary: Day below 0 °C (v)		
Others	**Day-of-Year (DOY)**	–	Non-spatial and daily
	Sampling Year	–	Non-spatial and yearly
	Sampling location (Basin-ID)	–	Spatial and static

and basin polygons. Following Steger et al. (2023), precipitation was represented using a short time window to capture triggering precipitation and longer time windows to account for antecedent precipitation. Triggering precipitation referred to the cumulative amount on the observation day and the preceding day, while antecedent precipitation was calculated over 7, 14, 21 and 30 d periods preceding the triggering precipitation. Mean annual precipitation over the 2005 to 2020 training period was included as a static baseline describing long-term spatial variability in precipitation. Daily mean temperatures and two binary indicators were used to mainly represent potential temporal temperature effects, while we emphasize that spatial temperature effects (i.e., differences between high elevations and valley bottoms) were likely to be only partially captured due to the basin-based landscape representation and the coarse resolution of the underlying CERRA data. The binary variables represent (1) whether the temperature crossed 0 °C on a given day, serving as a potential indicator for freeze-thawing and (2) whether the temperature remained continuously below 0 °C on a day, indicating potential frozen ground conditions. Finally, additional variables such as Day-Of-Year (DOY), sampling year and sampling location were included to account for seasonal patterns and group-level differences between sampling units.

4.3 Modelling within the core study area

The potential of mass movement impact was modelled for the core study area (Austria, South Tyrol) as a function of geo-environmental, exposure-related and meteorological variables using Generalized Additive Mixed Models (GAMMs). Separate models were fitted for each movement type, using parameter sets specific to the associated PPAs (Fig. 3d). GAMMs extend Generalized Additive Models (GAMs) by incorporating random group-level effects, while retaining the strengths of GAMs in modelling complex non-linear relationships through smooth functions, accommodating diverse error distributions and maintaining high interpretability. These characteristics make GAMMs particularly wellsuited to environmental modelling tasks (Zuur et al., 2009; Wood, 2017; Pedersen et al., 2019). Various versions of GAMs and GAMMs have been applied in data-driven landslide research (Goetz et al., 2015; Lombardo et al., 2018). In this study, the binary response was modelled using a binomial error distribution. The model was implemented using the bam() function from the mgcv package in R, which is specifically designed for modelling with large datasets (Wood et al., 2015; Wood, 2017). Variable selection was performed using an automated procedure based on double penalty shrinkage, which penalizes both the complexity of smooth terms to prevent overfitting and the null space to allow exclusion of non-informative predictors (Marra and Wood, 2011).

The modelling process began with a comprehensive initial variable setup (cf. variables in bold in Table 1) and proceeded iteratively, using automated variable selection throughout. To account for the hierarchical structure of the data, random intercepts were included for sampling year and sampling location. In the initial model, care was taken to avoid including multiple variables representing the same underlying effect. Specifically, only one variable for antecedent precipitation (based on a 30 d accumulation window) was included, while land cover and lithology were represented as categorical variables based on their dominant class within the PPAs. The resulting reduced models served as the basis for the next step, in which categorical land cover and lithology variables were supplemented with their continuously scaled counterparts (cf. Table 1) to assess whether additional information on the proportion of specific classes added value, both in terms of statistical significance (p-value < 0.05) and plausibility. For example, in the fall-type model, the proportion of bare surface was retained by the automated selection procedure, contributing significantly and exhibiting a plausible positive relationship, as higher proportions of bare surface within the PPA can reasonably be associated with increased rockfall activity.

The final step involved testing whether the initially selected 30 d accumulation window for representing antecedent precipitation was the best choice. This was evaluated using cross-validation (cf. Sect. 4.4.1), comparing the predictive performance of the 30 d model against alternative accumulation periods (7, 14 and 21 d), as well as against a null model that excluded antecedent precipitation entirely. As a result, one final model was selected for each movement type. For predictive mapping across the Alpine Space and performance assessment, predictions were based on fixed effects only, with random effects averaged (Wood, 2017).

4.4 Model evaluation

The modelling results were evaluated using multiple complementary approaches within the core study area covering Austria and South Tyrol. Model performance was assessed through cross-validation (Sect. 4.4.1). Variable importance assessment and inspection of partial effects provided insights into model relationships and supported plausibility checks (Sect. 4.4.2). Finally, modelled relationships were spatially transferred across the entire Alpine Space to generate daily spatial predictions for each basin (Sect. 4.4.3).

4.4.1 Assessing model performance within the core study area

The fitting performance of each model was evaluated on the training data by visualizing receiver operating characteristic (ROC) curves and calculating the area under the ROC curve (AUROC). The ROC curve illustrates the trade-off between the true positive rate (TPR) and the false positive rate (FPR) across different classification thresholds derived from predicted probabilities ranging from 0 to 1. The AUROC is a standard metric in binary classification that provides a single-number summary of the ROC curve, reflecting the ability of the model to distinguish between presence and absence observations. An AUROC of 1 indicates perfect discrimination, while a value of 0.5 corresponds to random guessing (Metz, 1978; Fawcett, 2006).

To evaluate predictive performance and identify the optimal antecedent rainfall time window, we employed 5-fold cross-validation with basin-based partitioning, repeated 10 times. Specifically, in each fold, 80 % of randomly selected basins were used as the training set to fit the model, while the remaining 20 % served as the test set for deriving the AUROC. Within each repetition, every basin was used once as a test basin and four times as part of the training set. Repeating this process across 10 independent random partitions resulted in 50 AUROC values per model (5 folds time 10 repetitions).

4.4.2 Assessing modelled relationships within the core study area

To enable model interpretation and plausibility checks of the internal model behaviour, we used variable importance assessment alongside visualization of partial effects. Variable importance, which quantifies the relative contribution of each predictor, was assessed using a permutation-based approach implemented in the R package vip (Greenwell and Boehmke, 2020). Specifically, for each predictor, values were randomly shuffled across the dataset, breaking the relationship with the response variable. The impact of this permutation on model performance was measured by the resulting decrease in AUROC. This procedure was repeated 100 times per predictor using Monte Carlo replications. Predictors causing a larger reduction in AUROC were interpreted as having higher relative importance in the model.

Partial effects plots complement variable importance assessment by providing insights into the modelled relationships at the single-predictor level. In the context of GAMs, partial effect plots graphically represent the estimated smooth functions that describe the relationship between the response and predictor variables (Simpson, 2024). In our study, these plots illustrate how the modelled effect of each predictor varies across its observed range, showing the contribution of that predictor to the overall prediction.

4.4.3 Creation of predictive maps within and beyond the core study area

A series of predictive maps and animations were produced by applying the modelled relationships from the three models within the validated core study area, as well as across the other, non-validated regions of the Alpine Space. The model predictions, expressed as probability scores, were spatially transferred to the basin level on a daily scale, excluding random effects and assigning a value of zero to trivial basins where no impacts are expected (i.e., where the PPA is absent or does not overlap with relevant infrastructure). In these maps, the probability scores do not represent absolute occurrence probabilities, but conditional probabilities influenced by the class balance in the training data (i.e., presence to absence ratio). Higher scores denote stronger resemblance to impact conditions, whereas lower scores indicate conditions typical of non-impact observations. It should be noted that the applications beyond the validated training domain serve as a technical demonstrator and are subject to important limitations. Predictions outside the core area should therefore be interpreted with caution, as they represent a non-validated similarity score indicating whether generalized local conditions resemble or differ from those associated with damage-causing landslides in the spatially distant training domain (cf. Sect. 6.4 and 6.5 for guidance on interpretation and relevance for operational implementation). As the model predictions are space- and time-specific, predictive maps were produced for selected constellations of dynamic variables. In this context, both "what-if" scenarios and hindcasting were employed to visualize model behaviour under hypothetical and real conditions, respectively.

In analogy to Moreno et al. (2024), a range of "what-if" scenarios were produced to depict how the model responds when subjected to controlled, hypothetical input settings. Specifically, a stepwise increase in precipitation, introduced through spatially uniform alterations of daily precipitation amounts, was used to evaluate how the estimated probability of mass movement impact varies across the Alpine region. Hindcasting involves simulating and analysing past conditions using a model originally designed to predict future outcomes. It is commonly employed to validate predictive models by comparing their outputs with known historical situations, thereby assessing their reliability and plausibility (Clement, 2011; Ozturk et al., 2021; Moreno et al., 2024). In our study, hindcasting was applied to well documented past events to explore model behaviour using historical input data and to illustrate its potential for application in an impact-based early warning context.

5 Results

5.1 Model performance within the core study area

The ROC curves (Fig. 5a) indicate relatively high fitting performance for all three models, particularly if considering that easy-to-classify observations were a-priori excluded. The flow-type model achieved the highest AUROC (0.9), followed by the slide-type (0.87) and fall-type (0.82) models. Points along each curve indicate the closest point to the top-left of the ROC space, representing the optimal thresholds that balance misclassification rates and best separate the two classes (Schisterman et al., 2005). At these thresholds, the slide-type model reached a true positive rate (TPR) of 0.78 and a true negative rate (TNR) of 0.81, the flow-type model achieved a TPR of 0.85 and TNR of 0.78 and the fall-type model a TPR of 0.78 and TNR of 0.72.

Cross-validation (Fig. 5b–d) was used to evaluate predictive performance and the influence of different antecedent precipitation time windows (7, 14, 21 and 30 d), alongside a null model without this variable. Median AUROCs were only slightly lower than their corresponding fitting performance (Fig. 5a), indicating a high predictive skill and limited model overfitting. For the slide-type and flow-type models, AUROC values increased more markedly with the inclusion of antecedent precipitation, whereas the fall-type model exhibited minimal variation across time windows, suggesting a weaker sensitivity to antecedent precipitation conditions.

The optimal time windows selected for the final models were 30 d for the slide-type model (median AUROC = 0.86), 21 d for the flow-type model (median AUROC = 0.89) and 14 d for the fall-type model (median AUROC = 0.80). Variability in predictive performance, expressed as the interquartile range (IQR) of AUROCs for the final models, can serve as an indicator of model stability, with higher IQRs denoting less consistent performance and greater uncertainty in generalization (Petschko et al., 2014). This variability was lowest for the flow-type models (IQR = 0.02), followed by the slide-type models (IQR = 0.03) and highest for the fall-type models (IQR = 0.05). While generally low across all three models, the variability indicates greater uncertainty in fall-type predictions while underscoring the relatively higher stability of the flow- and slide-type models.

5.2 Modelled relationships within the core study area

Permutation-based variable importance assessment revealed distinct patterns in the key factors influencing mass movement impact across the three models. The slide-type and flow-type models emphasize a combination of meteorological variables and static characteristics related to terrain morphology and exposure, whereas the fall-type model was dominated by static spatial variables, especially those related to exposure (Fig. 6).

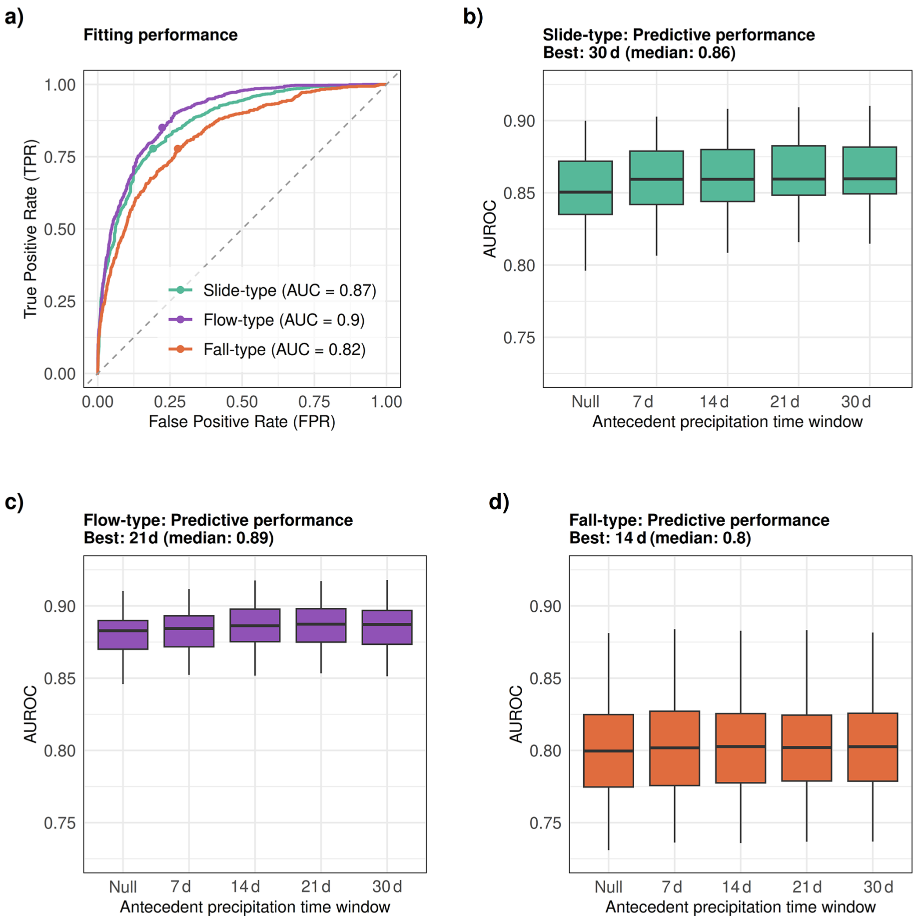

Figure 5. Model fitting performance and optimal cut-points based on the closest point to the top-left corner of the ROC space **(a)**. Predictive performances from basin-based cross-validation across different antecedent precipitation time windows are shown for the slide-type model **(b)**, flow-type model **(c)** and fall-type model **(d)**. Final models were constructed using the best-performing time windows: 30 d for slide-type, 21 d for flow-type and 14 d for fall-type.

For the slide-type and flow-type models, short-term precipitation, which served as a proxy for triggering rainfall, was the most influential variable, followed by mean annual precipitation. For the slide-type model, the next most important variables were mean slope angles, antecedent precipitation, the number of buildings in the PPA and the dominant lithology class within it. The flow-type model ranked mean daily temperature as the third most important predictor, followed by slope angle, antecedent precipitation and the number of buildings in the respective PPA. In contrast, the fall-type model showed a markedly different pattern, with static spatial factors dominating the top five ranks and short-term precipitation emerging only as the sixth most important variable. The most important predictors were exposure related, particularly the number of buildings and the extent of transport infrastructure within the fall-type PPA. Additionally, lithology, slope angle and the portion of bare surface were identified as relatively important factors.

Partial effect plots provided detailed insights into the modelled relationships between individual predictors and estimated impact potential at the single-predictor level (Figs. 7, 8, 9). When interpreting these plots, it is important to consider the relative importance of each predictor within the model (Fig. 6), distinguishing variables that are highly influential from those with lesser impact. For the slide-type model, the most important variable, namely short-term precipitation, showed a positive, non-linear association with estimated mass movement impact (Fig. 7a). The increase was steep and approximately linear up to 100 mm, after which the effect began to level off. The smooth term for antecedent precipitation indicated that lower precipitation amounts within the previous 30 d were associated with reduced estimated impact probabilities (Fig. 7b). Very high antecedent precipitation amounts exceeding 400 mm did not correspond to further increases in impact probability. Consistent with Steger et al. (2024), a clear negative relationship with mean annual precipitation was observed (Fig. 7c), indicating that basins

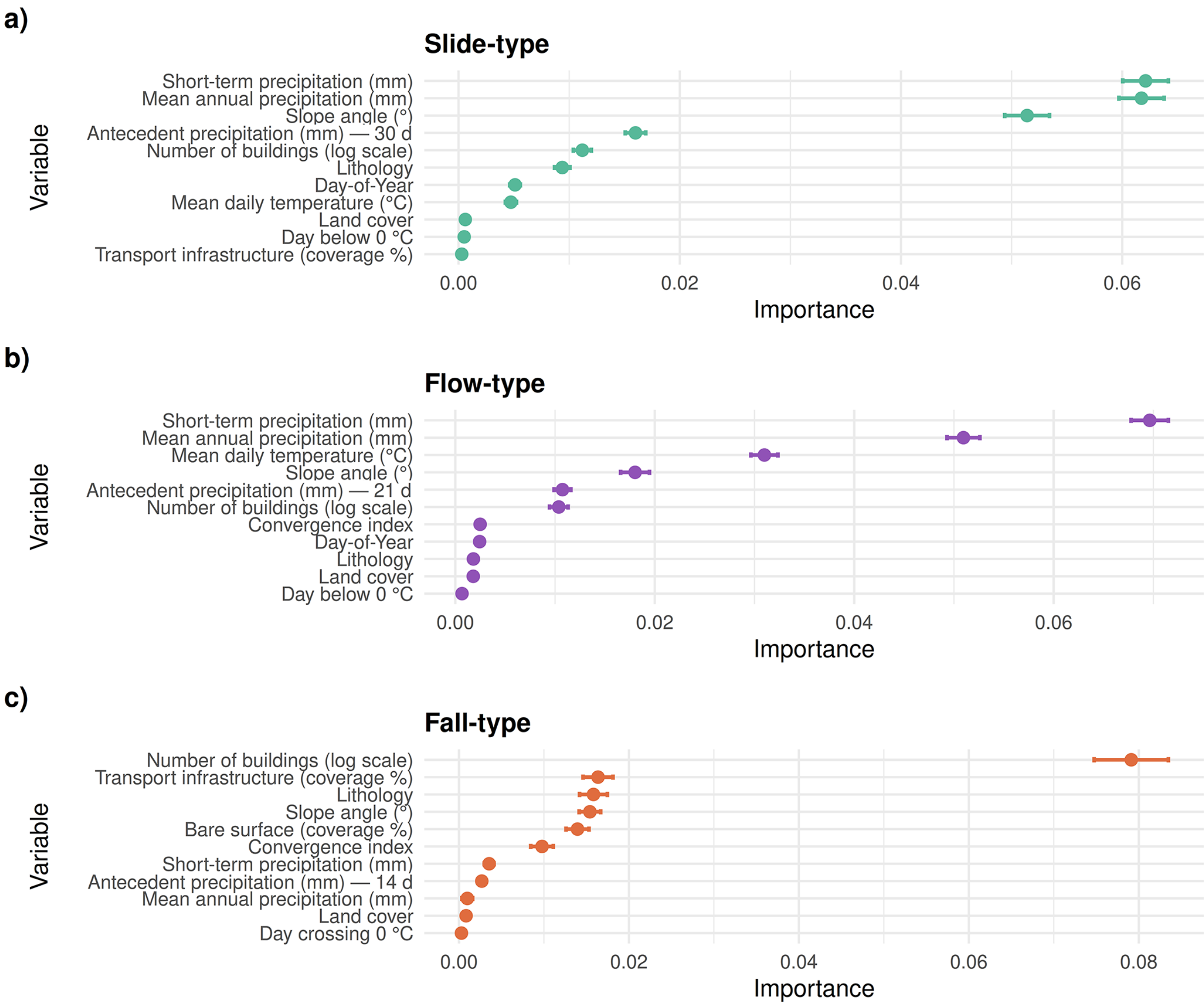

Figure 6. Permutation-based variable importance for the final three models, expressed as the decrease in AUROC after permuting each variable 100 times.

with generally drier conditions tend to respond more strongly to potential triggering events than basins adapted to wetter conditions. The potential for slide-type impact was higher in basins characterised by steeper terrain (Fig. 7d) and high exposure (Fig. 7e, f), indicated by the number of buildings and density of transport infrastructure within the potential slide-type terrain (PPA). Seasonal variation, modelled using a circular DOY effect, indicated that periods with reduced vegetation effects (i.e., winter, early spring) were associated with higher impact probabilities (Fig. 7g), noting that temperature and precipitation effects are accounted for by other variables in the model. Temperature variables revealed that particularly cold conditions below 0 °C corresponded to a lower impact potential, whereas hot days with mean daily temperatures exceeding 20 °C were associated with increased impact probabilities, suggesting that warmer "rainy" days, when convective events are more likely due to increased potential instability (Giorgi et al., 2016), may increase impact likelihood (Fig. 7h, k). Land cover and lithology showed partially significant differences among their classes, with basins dominated by deciduous forest and mixed carbonate lithology estimated to be more prone to slide-type impacts (Fig. 7i, j).

The flow-type models showed several patterns similar to those of the slide-type models. There was a clear positive relation between short-term precipitation and landslide impact (Fig. 8a), increased impact potential with higher antecedent precipitation (Fig. 8b) and a negative association with mean annual precipitation (Fig. 8c). Steeper slope angles and a higher number of buildings within the potential flow-type terrain (PPA) were further associated with higher impact potential (Fig. 8d, f). Seasonal effects, possibly related to vegetation periods, were again apparent (Fig. 8g). Notably, analogous to the slide-type model, mean daily temperature, the second most important predictor in the flow-type model, showed a strong positive relationship, likely reflecting the influence of rainfall-type, with warmer convective days increasing flow-type impact likelihood (Fig. 8h).

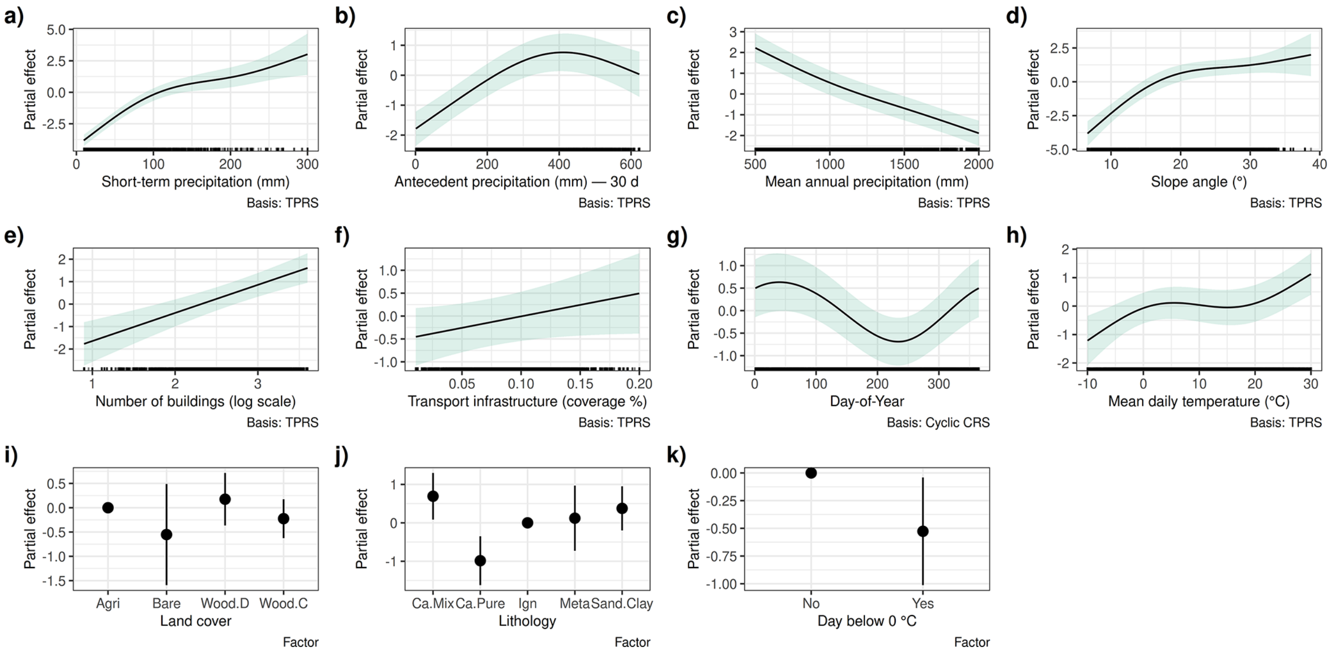

Figure 7. Partial effects for the slide-type model showing estimated smooth functions for continuous predictors and factor effects for categorical predictors, illustrating how each variable relates to modelled slide-type impact potential. Shaded bands indicate 95 % confidence intervals for smooth terms, while points with lines represent estimated effects and confidence intervals for factor levels. All effects are centered around zero. Higher values indicate a higher estimated likelihood of class membership (impact = yes), meaning that the higher the value, the higher the estimated probability of a slide-type impact.

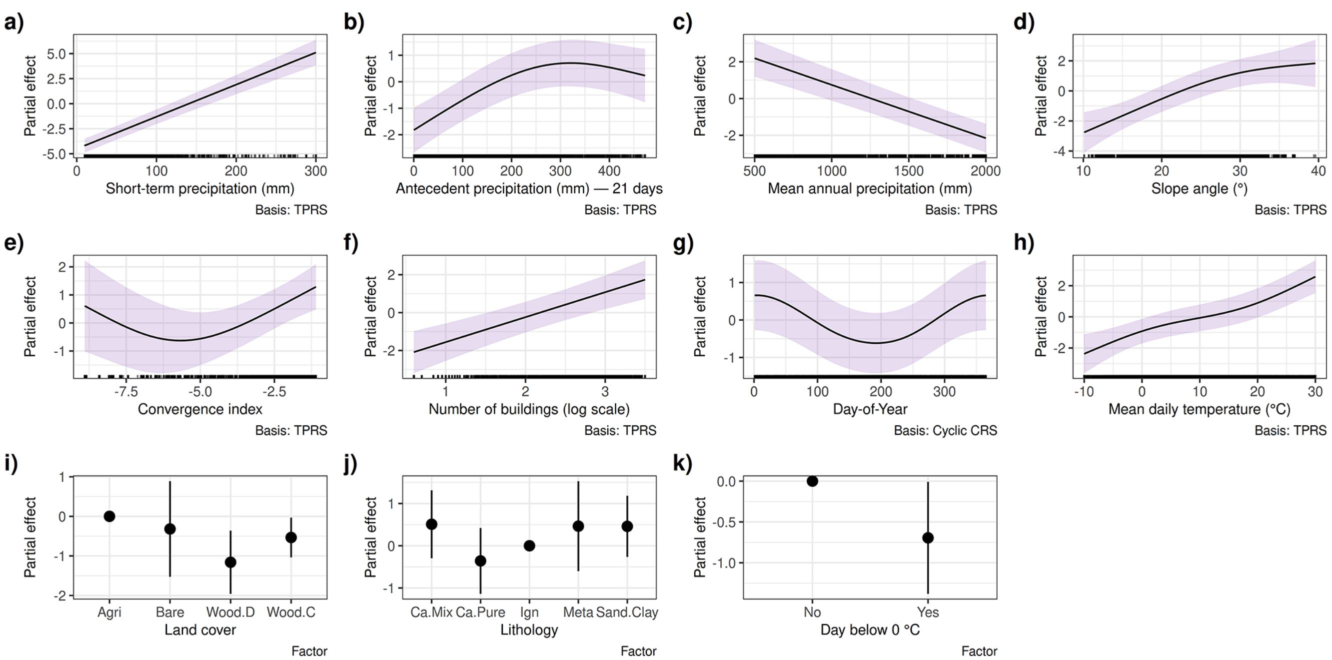

Figure 8. Partial effects for the flow-type model showing estimated smooth functions for continuous predictors and factor effects for categorical predictors. Shaded bands indicate 95 % confidence intervals for smooth terms, while points with lines represent estimated effects and confidence intervals for factor levels. All effects are centered around zero. Higher values indicate a higher estimated likelihood of class membership (impact = yes), meaning that the higher the value, the higher the estimated probability of a flow-type impact.

The fall-type model showed generally plausible relationships with meteorological variables (Fig. 9), although these variables were previously identified as less influential (Fig. 6). The two most important variables were static exposure factors, both exhibiting a positive relationship with estimated impact potential: when few buildings or a low density of transport infrastructure are present within the potential fall-type terrain (PPA), estimated impact probabilities are generally low (Fig. 9g, h). Slope angles within the fall-type PPAs were considerably steeper than those in the slide- or flow-type PPAs (cf. x-axis ranges in Figs. 9d vs. 7d and 8d). For fall-type models, impact potential increased continuously with slope steepness, whereas slide- and flow-type models showing a saturation effect at higher slope angles. Basins dominated by igneous and metamorphic rocks were estimated to be most prone to fall-type impacts (Fig. 9j) and a higher proportion of bare surface within PPAs further increased impact potential (Fig. 9f).

5.3 Maps and visualizations within and beyond the core study area

To explore model behaviour under controlled hypothetical conditions, "what-if" scenarios were visualized. The maps in Fig. 10 show model responses to spatially uniform increases in short-term precipitation of 20, 40, 80 and 160 mm, while all other dynamic variables were held constant. The zoom-ins provide a more detailed view of the predictions at basin level within the validated core study area. In line with the effects described in Sect. 5.2, slide-type and flow-type models responded strongly to increasing short-term precipitation (Fig. 10 top and middle rows). The fall-type model was comparatively less sensitive to this effect, with spatial patterns remaining relatively similar across precipitation scenarios (Fig. 10 bottom row). Because each basin was assigned the same short-term precipitation amount, the resulting prediction patterns reflect spatial differences in potential mass movement impact driven by geo-environmental and exposure characteristics. Across all models, the highest potential is concentrated in areas of steep terrain that coincide with higher densities of exposed assets.

Slide-type models generally indicate the largest spatial extent of potentially impacted areas, encompassing not only the high-relief regions of western Austria and South Tyrol but also extensive parts of the Austrian Alpine foreland in the east, where relief energy is comparatively moderate (Fig. 10d). In contrast, impacts from flow-type processes are less widespread and more strongly confined to steeper valley settings (Fig. 10i). Potential impact areas associated with fall-type movements are the most spatially restricted, with elevated values concentrated in high-relief zones of western Austria and South Tyrol, where buildings and transport infrastructure are frequently located within reach of steep rock faces (Fig. 10n).

Hindcasting was used to analyse model predictions under known conditions and to illustrate the output of the proposed framework. Storm Vaia (27 to 29 October 2018) served as an example of a severe, large weather event that affected multiple European countries. During the storm, heavy rain and strong winds caused extensive forest damage, flooding, and numerous damage-causing mass movements across the Alpine region (Cavaleri et al., 2019; Giovannini et al., 2021; Antonetti et al., 2022).

Figure 11 shows the model predictions for 29 October and for the storm aftermath on 2 November, along with precipitation variables. On 29 October, the potential for slide-type (Fig. 11a) and flow-type impacts (Fig. 11b) was estimated to be particularly high in northern Italy (South Tyrol, Trentino, Veneto, Liguria) and, to a lesser extent, in western Austria (Eastern Tyrol), southern Switzerland, southeastern France and northwestern Slovenia (Cavaleri et al., 2019; Menegatto et al., 2024). The precipitation maps indicate that this pattern was primarily driven by widespread, high precipitation amounts, with short-term precipitation being the dominant driver (Fig. 11d). Across most of the Alpine region, the 30 d antecedent precipitation did not exhibit exceptionally high values on 29 October, except in the southwestern regions (e.g., Liguria), where the precipitation front initially arrived (Fig. 11e). Notably, during this event, the highest precipitation occurred over mountainous terrain particularly prone to mass movement impacts, such as the western part of the core study area and adjacent regions to the south and west.

In contrast, in low-susceptibility regions, such as flat areas in Germany, localized heavy rainfall (Fig. 11d) did not lead to elevated estimated impact potential (Fig. 11a–c). Ultimately, high observed precipitation amounts without elevated impact potential indicate that the model also accounts for terrain susceptibility and the presence of exposed assets.

By 2 November, the estimated mass movement impact potential had generally decreased across the Alpine region, with more localised precipitation (Fig. 11i) still driving elevated predicted values in the southwest (Fig. 11f, g). Basins within the core study area no longer received high precipitation. However, they still exhibited moderate impact potential, primarily due to very high antecedent precipitation (Fig. 11j), which is used as a proxy for soil moisture conditions. Comparing both days for the fall-type model (Fig. 11c, h) further highlights its relatively low sensitivity to short-term weather dynamics.

In comparison to Storm Vaia, a more localised yet severe event struck the southeastern Alpine forelands from 23 to 26 June 2009. Triggered by thunderstorms associated with a low-pressure system over the Adriatic, the event led to more than 3000 mass movements of the slide- and flow-type, severely affecting transportation infrastructure and prompting the evacuation of several houses. The Austrian district Südosteiermark, at the centre of the affected area, sustained extensive damage, leading to the declaration of a state of emergency. Disaster response and reconstruction costs for

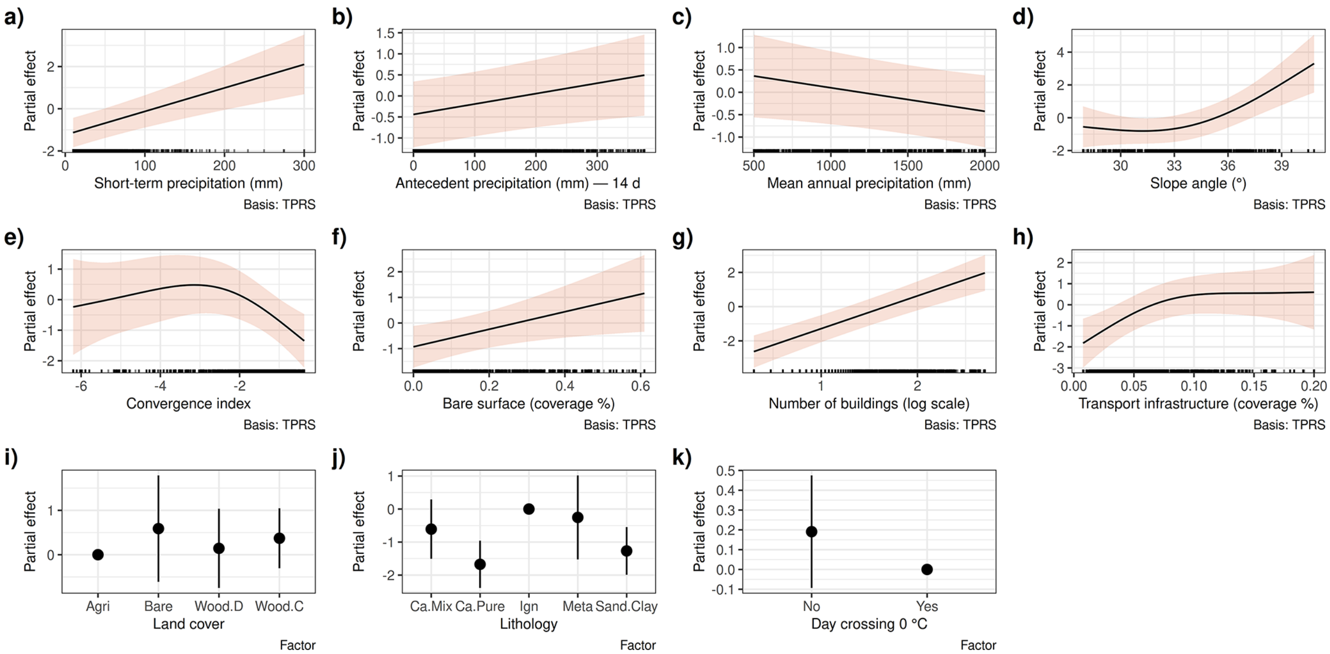

Figure 9. Partial effects for the fall-type model showing estimated smooth functions for continuous predictors and factor effects for categorical predictors. Shaded bands indicate 95 % confidence intervals for smooth terms, while points with lines represent estimated effects and confidence intervals for factor levels. All effects are centered around zero. Higher values indicate a higher estimated likelihood of class membership (impact = yes), meaning that the higher the value, the higher the estimated probability of a fall-type impact.

the state of Styria exceeded EUR 13.4 million (Hornich and Adelwöhrer, 2010; Maraun et al., 2022). Figure 12 shows the hindcast of this event for the slide-type model, along with the districts associated with the highest number of private damage reports.

According to Maraun et al. (2022), the precipitation event itself was severe, but not extreme. The exceptional mass movement occurrence has been attributed to the compounding effect of heavy rainfall combined with pre-moistening during the preceding winter and spring (Hornich and Adelwöhrer, 2010; Maraun et al., 2022; Mishra et al., 2023). Previous event-based landslide modelling for this area revealed that a 5 d rainfall variable was the strongest predictor, suggesting that also shorter-term antecedent conditions contributed to the observed mass movements (Knevels et al., 2020). Figure 12 shows the slide-type model hindcast for 25 June, with high estimated impact potential in the affected area largely matching the reported damage (Fig. 12a). For this model prediction, both high short-term precipitation (Fig. 12c) and elevated accumulated precipitation over the preceding 30 d (Fig. 12d) were key factors. Unlike the region-specific analyses by Maraun et al. (2022) the model did not capture pre-moistening at time scales beyond 30 d. Nonetheless, elevated wet conditions in June 2009 along the northern Alpine front led to widespread soil saturation and extensive flooding (Godina and Müller, 2009), likely influencing this mass movement event as well.

6 Discussion

The discussion Sect. 6.1 to 6.5 follow the main goals outlined in the introduction as well as model limitations, while Sect. 6.6 addresses the general transferability of the methodical framework and its potential application beyond impact-based early warning.

6.1 Capturing the interplay of impact drivers

The models were designed to estimate mass movement impact potential by integrating predisposing, preparatory and triggering conditions represented through meteorological, geo-environmental and exposure data. Separate models were generated for each movement type, because different landslide types are driven by distinct sets of conditions (Loche et al., 2022).

Regarding dynamic variables, the slide- and flow-type models are highly sensitive to daily changes, whereas fall-type models are heavily governed by static spatial variables. For slide- and flow-type models, the most important predictor of potential impact to infrastructure is short-term “triggering” precipitation. Antecedent precipitation, DOY, and temperature also have an important contribution, reflecting soil moisture, seasonality, and temperature effects. For instance, in the flow-type model, mean daily temperature ranked as the second most important predictor, with hot days showing the highest impact potential, likely due to an increased potential

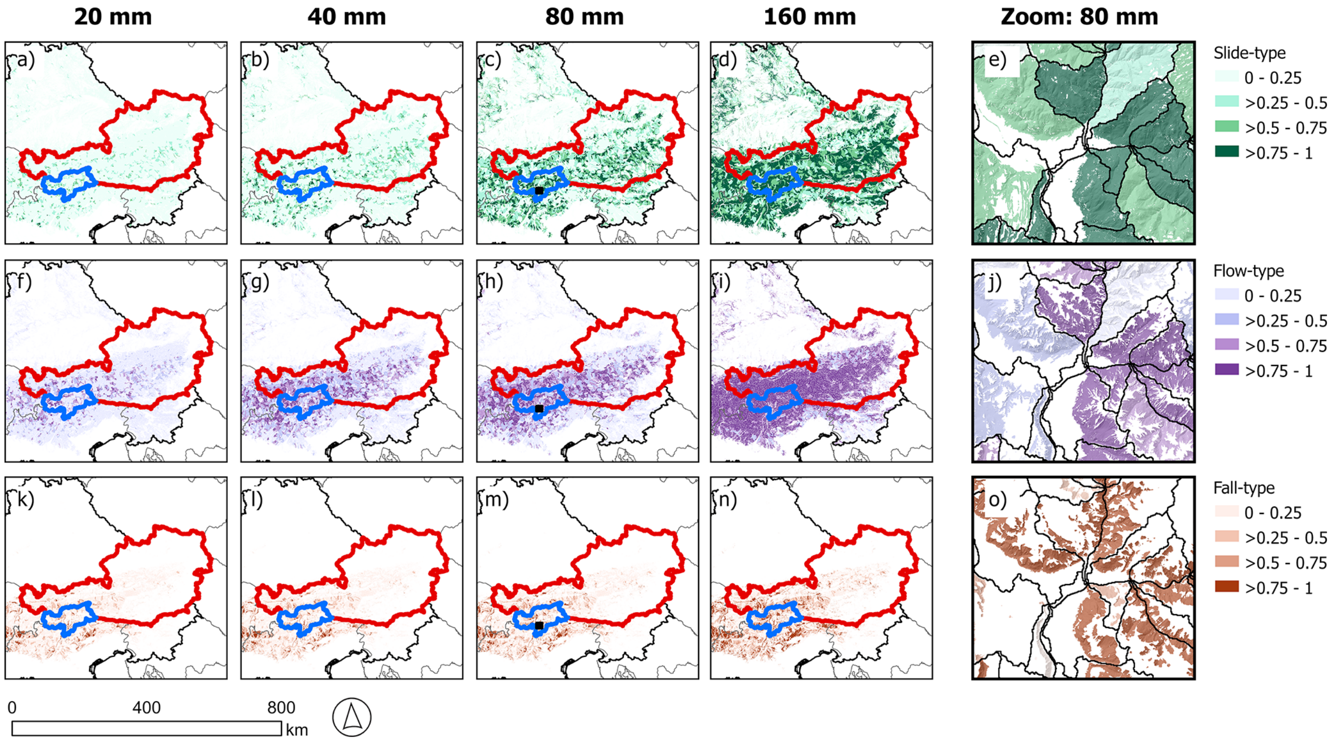

Figure 10. Visualization of "what-if" scenarios for slide-type models **(a–e)**, flow-type models **(f–j)** and fall-type models **(k–o)** under spatially uniform increases in short-term precipitation. The figure depicts the core study area (red: Austria; blue: South Tyrol) and a portion of the surrounding Alpine Space. Shown are model predictions for "triggering" precipitation amounts of 20, 40, 80 and 160 mm, with all other dynamic variables held constant (antecedent precipitation = 50 mm, mean daily temperature = 20 °C, Day-of-year = 200, binary temperature = "Above 0 °C" and "Not crossing 0 °C"). The zoom-in panels depict the 80 mm "triggering" precipitation scenario. Animations showing precipitation increases in 10 mm increments from 10 to 200 mm are provided in the video material for each movement type (Steger, 2025; S1–S3 at: https://doi.org/10.6084/m9.figshare.30271795).

of convective activity (Giorgi et al., 2016), while days below 0 °C were associated with the lowest impact likelihoods, possibly reflecting frozen ground effects on slope stability. The range of dynamic variables shows that the models captured effects across multiple temporal scales. This finding is in line with previous studies that show mass movement occurrence depends also on antecedent conditions over longer periods (Crozier, 1999; Mirus et al., 2018; Rosi et al., 2021; Maraun et al., 2022; Smith et al., 2023).

In this context, daily precipitation and temperature variables were assumed to represent short-term conditions, antecedent precipitation captured cumulative effects over preceding weeks, and the DOY variable reflected seasonal influences, primarily related to vegetation (Steger et al., 2023), since other season-related meteorological effects were already accounted for. However, it should be noted that the interpretation of individual predictor effects remains challenging, as confounding between variables (e.g., temperature, elevation, and DOY), along with specific biases in landslide inventories, can strongly influence the measured effects and limit a straightforward physical attribution, as discussed in Steger et al. (2021). Although model performance was generally high (Fig. 5), better capturing environmental dynamics could further improve their explanatory power. For example, instead of relying on proxies, soil moisture data derived from simulations or hydrological modelling could better capture actual soil wetness conditions (Maraun et al., 2022), while considering information on sediment availability may further enhance the model (Heiser et al., 2023). Incorporating information on specific precipitation and weather types to explicitly distinguish convective events from other weather dynamics could further improve the representation of rainfall-triggering conditions, making the models less reliant on proxies, such as dynamic temperature effects. Also, precipitation data at sub-daily resolution would likely capture actual rainfall triggering conditions more accurately, particularly for rapid flow-like events (Marra et al., 2016). In such case, sub-daily mass movement occurrence data should ideally be available to match this high-resolution data. When such detailed observations are lacking, aggregating sub-daily rainfall to daily scales by using e.g., the maximum 3 h rainfall intensity on a day, has been shown to be of value (Knevels et al., 2020; Smith et al., 2023).

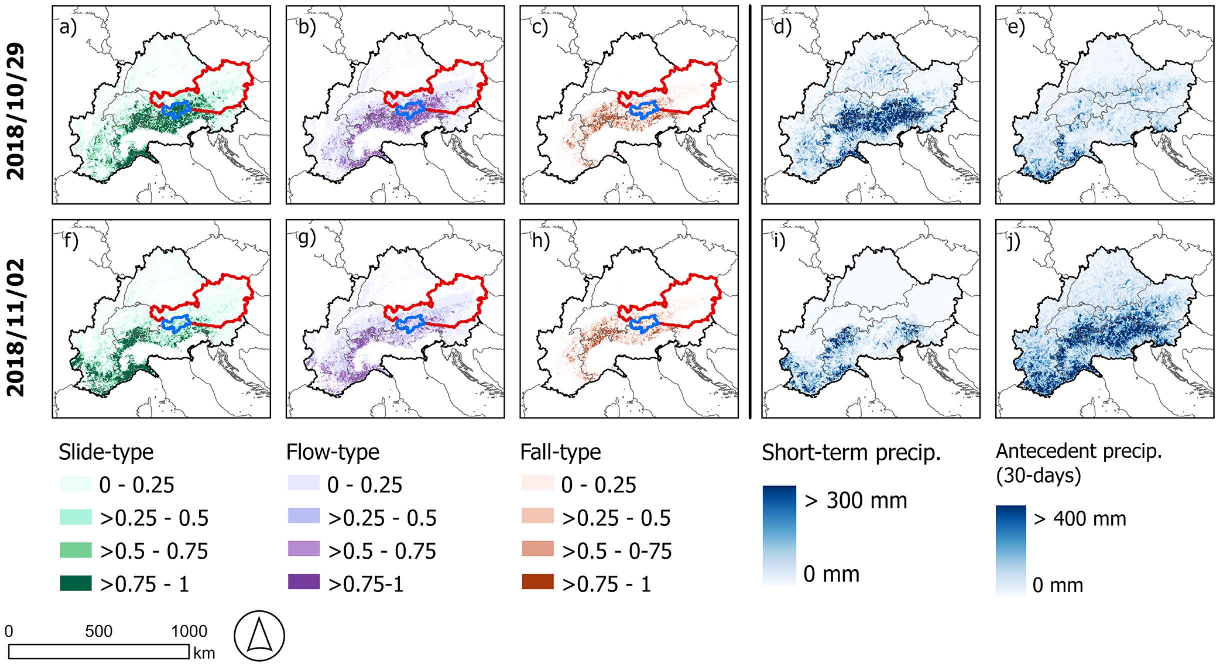

Figure 11. Hindcast example of Storm Vaia for the core study area (red: Austria; blue: South Tyrol) and the surrounding Alpine Space (regions outside the red and blue polygons). Model predictions for 29 October (top row) and the aftermath on 2 November (bottom row) for three movement types: slide-type **(a, f)**, flow-type **(b, g)** and fall-type **(c, h)**. Corresponding precipitation variables for the same dates are shown, including short-term precipitation as used within all models **(d, i)** and antecedent 30 d precipitation as used for the slide-type model **(e, j)**. Note that the model was calibrated and validated only within the core study area (red and blue polygons). Predictions outside this area reflect the similarity of generalized local conditions to those causing damage-inducing landslides in the core area (values close to 1 indicate higher similarity, values close to 0 lower similarity). Hindcast animations of this event are provided in the video material (see Steger, 2025; S4–S6 at: https://doi.org/10.6084/m9.figshare.30271795).

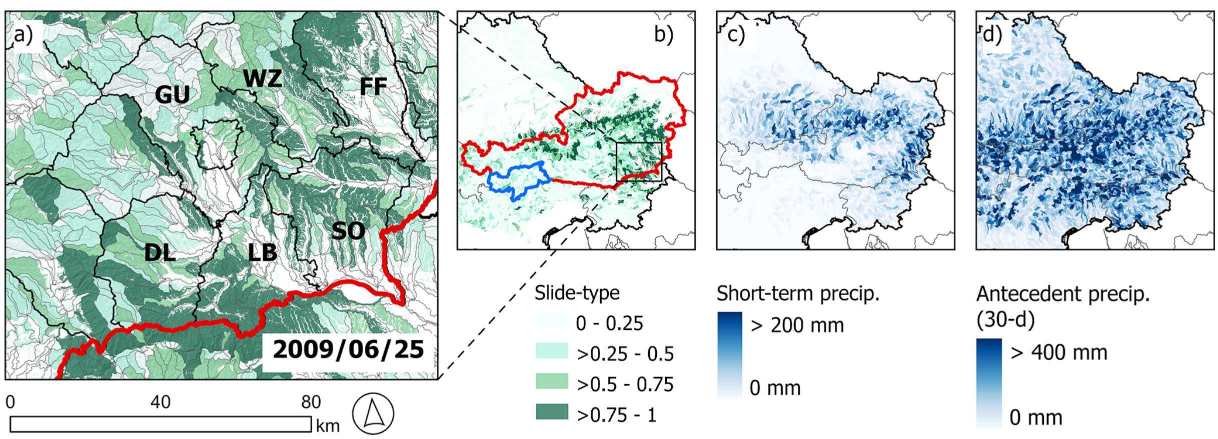

Figure 12. Hindcast example of a severe event in Styria, Austria. Model predictions from the slide-type model for 25 June 2009, are shown for the focus area of the event **(a)** and the calibration area of Austria (red in **b)** and South Tyrol (blue in **b**), together with the variables representing short-term precipitation **(c)** and 30 d antecedent precipitation **(d)**. Black polygons in **(a)** delineate the districts of Styria, with labels showing the districts linked to the most private damage reports: Südoststeiermark (SO, 600 reports), Leibnitz (LB, 324), Weiz (WZ, 287), Graz-Umgebung (GU, 205), Deutschlandsberg (DL, 95) and Fürstenfeld (FF, 62) according to Hornich and Adelwöhrer (2010). Hindcast animations of this event are provided in the video material (see Steger, 2025; S7 at: https://doi.org/10.6084/m9.figshare.30271795).

Depending on the modelling context, potential enhancements in the dynamic component include snowmelt, vegetation seasonality, season-dependent precipitation windows, functional precipitation representations, and interactions with other geo-environmental variables (Krøgli et al., 2018; Schmaltz et al., 2019; Moreno et al., 2025). In addition, modellers could also treat land cover and exposure as dynamic variables to capture long-term changes, such as forest disturbance (Pisano et al., 2017; Pittore et al., 2017; Sebald et al., 2019; Pacheco Quevedo et al., 2023). Yet, while many opportunities exist to better represent dynamic processes, early warning applications benefit from parsimony, not least because suitable input data are often limited (Stähli et al., 2015; Kaltenberger et al., 2020; Potter et al., 2021). In our context, relying on scalar precipitation variables and a date-derived proxy (DOY) strikes a practical balance, ensuring feasibility as well as compatibility with the lead times of existing precipitation nowcasts and forecasts.

All models relied on several static spatial variables, with the fall-type model being the most strongly influenced by them (Fig. 6). Consequently, for the fall-type model, it was generally easier to estimate where impacts might occur than when. Given the scale of this investigation, this result is plausible, as potential impact locations for fall-types are generally confined to basins with steep terrain and downslope exposed assets. In contrast, the timing of a fall-type movements is inherently complex to predict, particularly at these scales and when relying solely on meteorological variables. Accordingly, rock fall warning often relies on local sensors or remote sensing techniques that monitor rock faces for precursors of failure (Stähli et al., 2015). For the fall-type model, the two most influential predictors were exposure-related, with the number of buildings clearly dominant. While slope angle might intuitively be expected to dominate at this scale, its effect was largely accounted for by the PPA delineation (Fig. 3).

To move from a purely process-oriented to an impact-based perspective, exposure information was incorporated in two steps, allowing the modelling framework to move beyond conventional landslide early warning approaches (Guzzetti et al., 2020). First, the modelling domain was limited to basins where PPAs coincided with infrastructure. Second, within these basins, exposure variables based on building counts and road networks were included. Across all models, the relationships consistently showed that higher exposure increases potential impact. However, despite careful efforts to prepare representative impact data, we cannot fully exclude the possibility that the estimated exposure effects are partly confounded by inventory-related biases or by elevated landslide occurrence in the vicinity of infrastructure resulting from increased human interventions and construction activities (Steger et al., 2021).

However, a key component of risk, namely the vulnerability of infrastructure to the mass movement processes, is missing in our approach. At this scale, incorporating structural vulnerability is challenging (Caleca et al., 2025), as event data lack damage and hazard intensity information, and the model outputs and exposure data are insufficient to apply damage functions. Furthermore, technical mitigation measures, such as torrent control structures (e.g., check dams and rockfall netting), which are widely implemented in alpine regions to mitigate gravitational natural hazards, were not accounted for in this analysis. By stabilizing slopes and regulating water and sediment flow, these structures reduce hazard intensity and protect downstream infrastructure. Their omission may therefore lead to an overestimation of potential impacts (Schlögl et al., 2021).

Besides exposure-related effects, all models showed the highest estimated impact potential in basins with relatively steep terrain (slides and flows) or very steep terrain (falls), particularly in areas with low mean annual precipitation. The negative relationship with mean annual precipitation was most pronounced in the slide- and flow-type models, consistent with previous modelling results (Steger et al., 2024). This suggested that landscapes with higher long-term precipitation (e.g., 2000 mm yr^{-1}) may be better adapted to wet conditions and therefore less responsive to individual events, unlike drier basins (e.g., 500 mm yr^{-1}). These results therefore provide quantitative support for the landscape equilibrium hypothesis (Renwick, 1992; Smith et al., 2023).

Although we aimed to produce plausible results through a tailored and innovative landscape representation (Sect. 6.2), a carefully designed sampling strategy (Sect. 6.3), and enhanced model interpretability (Sect. 6.4), the above process-oriented interpretations should nevertheless be approached with caution. In data-driven landslide modelling, particularly under data bias conditions, correlation does not necessarily imply geomorphic causation (Steger et al., 2021). An underlying reason for this limitation is the frequent lack of consistent and comprehensive landslide inventory data used for model training. This issue becomes particularly critical for very large-area assessments (e.g., at the European scale), where the integration of heterogeneous datasets from different sources poses additional challenges (Caleca et al., 2025).

Even within comparatively well-studied regions, such as the training domain comprising Austria and South Tyrol, mass movement inventories exhibit considerable inconsistencies and pronounced biases that can influence modelling results (Lima et al., 2021; Steger et al., 2021). In particular, the inventories used in this study are affected by positional inaccuracies, which were addressed through a generalized landscape representation (Sect. 6.2), as well as by a systematic underrepresentation of slope instabilities that did not result in damage. This limitation substantially reduces their suitability for purely process-oriented mass movement analyses, as events occurring in remote areas are typically not systematically recorded (Trigila et al., 2010; Heiser et al., 2019; Steger et al., 2021). In line with previous modelling approaches focusing on damage-causing landslides (e.g., Steger et al., 2021), the present study is assumed to be less adversely affected by such spatial bias, as it explicitly targets mass movement impacts, which are generally mapped more consistently in the datasets. This shift in focus is expected to enable a more targeted identification of areas where landslides are likely to cause damage. In other words, by redefining the modelling objective, from general mass movement occurrence to areas and time periods likely affected by damaging events, the approach leverages characteristics of the underlying data that would otherwise be considered detrimental biases. Thus, in this modelling context, the focus of the inventories on damage-causing events becomes advantageous rather than limiting, as it enhances, together with a targeted landscape representation, the ability of the approach to systematically identify areas with impact potential.

6.2 Accounting for mass movement runout paths while maintaining a generalized landscape representation

Data preparation aimed to balance landscape generalization with sufficient detail. This involved the delineation of basins and the definition of process-relevant terrain (i.e., PPA) within each basin. Pixel-based runout information was incorporated into the basin-based model framework to combine the stability and reduced noise of basin-scale units (Alvioli et al., 2016; Loche et al., 2022; Woodard et al., 2024) with the spatial detail relevant to capture mass movement propagation and impact.

Basins were chosen as the main spatial unit to overcome limitations of high-resolution raster representations. Basin-based units can mitigate uncertainties in landslide positional accuracy, reduce computational demands for large-area prediction tasks, and allow flexible aggregation of input variables (e.g., averages, dominant classes, proportions) (Alvioli et al., 2016; Woodard et al., 2024). Such units can also reduce the impact of errors or changes in predictor data. For instance, moderately pronounced changes in variables like forest cover or building counts are likely to have little effect on aggregated basin values, whereas in pixel-based models, individual cells and therefore subsequent model predictions may deviate substantially.

However, this increased generalization also has potential drawbacks. Aggregating properties across entire basins can obscure important details, as predictor variables may no longer reflect conditions where processes are most relevant. For instance, phenomena linked to very steep terrain, such as rockfalls, may not be captured by a mean slope over a basin. Similarly, in exposure or risk assessments, assets beyond the actual reach of mass movements may be incorrectly counted as exposed or contributing to risk (Caleca et al., 2025). We argue that pixel-based representations, despite having some disadvantages, also offer advantages in capturing fine-scale spatial variability. This study aimed to combine the benefits of both approaches, preserving sufficient landscape generalization while retaining the spatial detail suitable for capturing mass movement impact. Delineating PPAs separately for each movement type enabled integration of pixel-based runout information into basin-level representations (Fig. 3), providing a more realistic depiction of process-relevant geoenvironmental conditions and particularly of potentially exposed assets. Nonetheless, the approach remains constrained by uncertainties inherent in the simplified runout modelling procedure and does not replace site- or catchment-specific analyses (Mergili et al., 2015; Wichmann, 2017). In summary, this innovative method mitigates several drawbacks recently highlighted in large-area landslide susceptibility, exposure, and risk assessments (Lima et al., 2021; Loche et al., 2022; Lin et al., 2023; Marchesini et al., 2024; Caleca et al., 2025).

6.3 Avoiding oversimplified patterns through tailored sampling

A wealth of studies on data-driven mass movement modelling highlight that the quality of input data is directly reflected in the quality of the resulting models, reinforcing the widely recognized maxim of “garbage in, garbage out” (van Westen et al., 2008; Petschko et al., 2014; Steger et al., 2016b; Reichenbach et al., 2018; Lima et al., 2022; van Natijne et al., 2023). A less frequently addressed and equally important issue concerns how available input data should be sampled before being included in a data-driven model (Dornik et al., 2022; Rabby et al., 2023; Guo et al., 2024). Data sampling design plays a decisive role in ensuring that models capture relationships beyond those that could be anticipated by common sense. Designing such strategies is a non-trivial task, particularly in the context of space-time modelling, where computational feasibility, data considerations (e.g., group-effects, autocorrelation) and content-related aspects need to be considered (Steger et al., 2024).

In space-time modelling, sampling design must carefully account for both spatial and temporal dimensions. Spatially, this entails selecting appropriate locations from which training data are drawn. Temporally, sampling must ensure periods are captured that are relevant to the processes under study. If, for example, the present study had relied on a pixel-based approach with random sampling of absences without further restriction, the resulting models would likely have reflected trivial distinctions, separating flat terrain from hillslopes or dry from rainy days, rather than the conditions most relevant for decision-making (Steger et al., 2023, 2024). Previous studies show that such “oversimplified” models may appear to perform well statistically, as distinguishing mass movement presences from randomly drawn, largely irrelevant absences can be straightforward. Guo et al. (2024) showed that sampling absences far from known mass movements, using larger buffer distances, increases dissimilarity between presence and absence observations, thereby boosting measured model performance and suggesting improved model quality. From our viewpoint, however, such sampling leads to the opposite effect, as it forces absences into trivial terrain, artificially inflates performance, and promotes oversimplified models with limited decision-making value (Steger and Glade, 2017).

In this study, we avoided sampling in terrain irrelevant to mass movement impacts. Presence and absence observations were restricted to basins where exposed assets (buildings, roads) fall within PPAs, focusing the modelling on areas with realistic impact potential. For instance, fall-type sampling targeted steeper Alpine basins, while slide-type sampling was less constrained, covering much of the Alpine foreland. Similar considerations guided the temporal sampling. To reduce trivial temporal contrasts, sampling was restricted to days with at least moderate rainfall, defined using an arbitrary threshold of $10\,\mathrm{mm\,d^{-1}}$. In our earlier studies (Moreno et al., 2024; Steger et al., 2024), a much lower threshold was used ($1.1\,\mathrm{mm\,d^{-1}}$) to include only rainy days while accounting for data uncertainty. Focusing on at least moderate rainfall aimed to better align the models to decision-making contexts, where light precipitation is less relevant. Threshold choice also affects the similarity between presence and absence samples, influencing estimated modelled relationships and model performance scores. For example, limiting absence sampling to heavy rainfall days ($> 40\,\mathrm{mm\,d^{-1}}$) would likely reduce the discriminative power of short-term precipitation, lowering variable importance and overall model performance. More broadly, the distinction between relevant and irrelevant input data depends on modelling objectives while associated implications apply to both spatial and temporal sampling.

Literature contains numerous examples of exceptionally well-performing landslide susceptibility models. While there are valid cases of well performing models with appropriate sampling strategies, we assume that in many instances, models rely on oversimplified classification tasks, arising either from unrestricted random sampling or from sampling that even forces absences to overrepresent trivial observations (Zhu et al., 2019; Rabby et al., 2023; Guo et al., 2024). Scepticism toward apparently well-performing landslide models is not new (Hearn and Hart, 2019; Steger et al., 2016a). We assume that, in essence, the root causes of this criticism can often be traced to the underlying sampling design, which leads models to make overly simplistic distinctions that provide limited practical value for decision support. In space-time modelling, this issue can be amplified, as trivial observations may be sampled not only across space, but also over time or simultaneously in both.

6.4 Added value of model explainability and suitability for impact-based warning

Another important aspect for enhancing model utility is interpretability, particularly when results are intended to support decision making. Many machine learning studies in landslide research emphasize performance metrics, often at the expense of geomorphic plausibility and interpretability. This can limit operational uptake, since end-users benefit more from models that are interpretable, plausible, and trustworthy (Lombardo et al., 2020; Collini et al., 2022; Nocentini et al., 2023; Caleca et al., 2024). Using interpretable models (Maier et al., 2024; Molnar, 2025) is valuable for communicating findings to users and internal plausibility checks, as well as model refinement. From an application perspective, we argue that prioritizing predictive performance is not always ideal, as less performant but more interpretable models can be more useful in practice. In this study, particular attention was given to model interpretation, using GAMMs to visualize non-linear relationships between predictors and the response, alongside variable importance assessments. Combined with hindcasts and "what-if" scenario analyses, this facilitated a clearer understanding of model response.

In terms of applicability for impact-based warning contexts, the proposed modelling framework and the results of the slide- and flow-type models demonstrate potential for large-area applications within the core study area. The fall-type model, in contrast, is less sensitive to short-term variations in weather conditions. Consequently, its utility for early warning appears limited. The lower number of presence observations, together with the more pronounced class imbalance between presences and absences (647 vs. 3422; 19 %), may contribute to the reduced performance of the fall-type model. However, the prevalence of presence observations still remains within a range (> 10 %) commonly considered sufficient for model fitting (Steen et al., 2021).

Potential operational uptake of the models also depends on the meteorological input data. All models were trained on a consistent set of inputs derived from CERRA reanalysis (Ridal et al., 2024). Regarding applicability, it should be noted that precipitation data from reanalyses used to train the models may differ from the data available in nowcasting or forecasting systems. Such potential biases should be addressed prior to operational implementation, for example through bias correction or the use of alternative meteorological inputs, to reduce discrepancies between model training and operational datasets. Ideally, data perfectly consistent with nowcasting or high-resolution forecasting would be used for model training. In practice, however, such data often lack long-term historical coverage or exhibit temporal inconsistencies due to changes in operational forecasting systems, limiting their suitability for model training over extended periods. Nevertheless, building the model on precipitation data with higher-than-daily temporal resolution could further improve the models, as discussed in Sect. 6.1.

Furthermore, real-time application would additionally require an automated workflow to integrate near-real-time meteorological data and deliver timely model outputs. While this was beyond the scope of the present study, it represents an important step for future work and operational uptake. An additional limitation for operational application is that the performance of the spatially transferred model predictions could not be quantitatively assessed beyond the spatial training domain (Fig. 1) due to the lack of time-stamped landslide data containing explicit information on infrastructure impacts (Sect. 6.5). Qualitative hindcast analyses, however, provide indication of model plausibility, while future refinements and quantitative evaluation could be achieved using spatially consistent impact data across the entire area.

6.5 A word of caution: Interpreting probability scores within and beyond the training domain

Another important consideration when interpreting the presented model predictions concerns the spatial domain in which the models were trained and validated versus the regions to which they are applied (Fig. 1). The models were calibrated and quantitatively validated exclusively within the 91 000 km^2 core study area (Austria and South Tyrol). Consequently, predictions generated outside this domain constitute non-validated spatial extrapolations. In these regions, model outputs should not be interpreted as reliable impact estimates, but rather as a basic indicator of the similarity between generalized local conditions and those associated with observed impact-generating events within the distant training domain. The lack of consistent inventory data for large areas (cf. Sect. 6.1) becomes even more critical beyond the widely applied landslide susceptibility context, particularly in impact-based spatio-temporal modelling, where not only the location of past events is required, but also their timing and, crucially, associated damage information. Accordingly, future improvements and a more robust transfer of modelling approaches to the Alpine-wide scale would benefit from the development and harmonization of time-stamped, impact-oriented landslide inventories across the Alpine arc.

Given that even compiling consistent process inventories at such scales is associated with substantial uncertainties (Caleca et al., 2025), this is likely to remain a challenging and resource-intensive task. Therefore, we emphasize promising methodological advances that explicitly address the transfer of model-derived information from well-investigated domains to data-sparse domains. In particular, transfer learning techniques, combined with spatially explicit model tuning and validation strategies, offer valuable pathways to improve model transferability and enhance the robustness of predictions under persistent and difficult-to-overcome data limitations (Wang et al., 2022; Schratz et al., 2024; Brenning and Suesse, 2026).

A further important aspect concerns the interpretation of the predicted probability scores, also within the core study area where the model was trained and validated. These values do not represent absolute probabilities of impact occurrence, but conditional probabilities influenced by the class balance of the training data. Given that absence observations substantially outnumber presence observations in our dataset, the predicted probabilities are generally biased toward lower values. Moreover, the raw probability scores produced by the different model variants are not directly comparable, as they are derived from datasets with differing presence-to-absence ratios. Misinterpretation of these scores may hinder user uptake and reduce trust. For instance, a value of 0.7 should not be interpreted as a 70 % likelihood of a mass movement impact occurring in a given basin on a specific day. Instead, higher values indicate greater similarity to conditions associated with observed impact events within the model training domain, whereas lower values reflect greater similarity to non-impact conditions. For practical application in impact-based warning systems, these continuous similarity scores would need to be transformed into discrete warning levels (e.g., red, orange, yellow). While objective thresholding approaches based on performance metrics such as true positive and false alarm rates exist (Steger et al., 2024), their effective implementation requires careful calibration against independent data and, ideally, co-development with end-users. Incorporating local knowledge and context-specific requirements is essential to ensure that derived warning thresholds are both interpretable and actionable (Budimir et al., 2025). Overall, while the presented modelling framework shows clear promise for data-driven, impact-based warning, the operational usefulness of the resulting models remains limited at the current stage of development. This is particularly the case beyond the training domain.

6.6 Transferability of the approach and potential applications beyond impact-based early warning

The methodological framework presented in this study can be adapted to develop dynamic, spatially explicit impact models for other phenomena and regions. Beyond mass movement impacts, it may also be applicable to other rapid-onset hillslope processes, such as flash floods or snow avalanches, as well as to hazards like wildfires or hail, where impacts result from multiple drivers acting across scales. Key aspects include a tailored yet generalized landscape representation that accounts for spatial uncertainty in input data, for process propagation dynamics, and integration of meteorological, geo-environmental, and exposure/vulnerability information. Targeted sampling to avoid trivial observations is emphasized to ensure meaningful model patterns, while model interpretability can support plausibility checks and effective result communication.

Beyond impact-based early warning, this framework can also support the analysis of spatio-temporal patterns and trends over extended areas and periods. For instance, the models developed in this study are intended to produce thousands of daily hindcasts at the basin scale, supporting multi-decadal analyses of patterns. Averaging these hindcasts at the basin level can extend conventional landslide susceptibility and exposure assessments, which typically do not capture the spatio-temporal dynamics of meteorological drivers. A large number of hindcasts can also be used to analyse the frequency of threshold exceedance per basin or to conduct trend analyses, revealing systematic shifts in impact potential over time. In the context of climate impact assessment, the models can, in principle, be adapted to digest climate projection data. Since the models can also be adapted to work with sub-daily inputs, the ongoing tendency in climate modelling toward producing sub-daily information over extended areas and periods (Fosser et al., 2015, 2024) might open avenues for sophisticated climate impact analysis. Nevertheless, potential limitations, such as the "drizzle bias" (overestimation of weak and underestimation of heavy precipitation) and the spatial skill scale, must be considered when applying climate projection data in high-resolution spatio-temporal modelling (Benestad et al., 2019; Lazoglou et al., 2024).

7 Conclusions

This study presents a comprehensive, dynamic, and spatially explicit modelling framework for the impact-based assessment of mass movements across large areas. By addressing key limitations of traditional static susceptibility approaches, the framework integrates geo-environmental, exposure, and dynamic meteorological data into a unified modelling strategy. Process-specific models for slide-, flow-, and fall-type movements capture distinct spatio-temporal patterns and provide interpretable outputs that can support risk-informed decision-making within the training domain. The primary contribution of this work lies in the development of a transferable methodological framework rather than an operational early warning system. While the slide- and flow-type models demonstrate encouraging potential for application in an early warning context within the training domain, their operational use remains constrained and requires further development. The fall-type model, in particular, shows limited sensitivity to meteorological forcing and therefore bearing more the character of an almost static spatial assessment.

To our knowledge, this study presents the first implementations of an impact-based mass movement modelling framework that is explicitly process-specific and integrates geo-environmental, exposure, and weather information across scales. Its adaptability to other hazards, compatibility with climate data, and applicability across regions highlight the versatility of the framework and its broader potential for disaster risk reduction and climate impact assessment.

Code and data availability. The R code for model training and basic visualizations, along with the associated training data, the outline of the Alpine Space and the basin delineation, is available on GitHub at https://github.com/StefanSteger/LandslideImpact_AlpineSpace_NHESS (last access: 28 July 2026, released on Zenodo via https://doi.org/10.5281/zenodo.21645145, Steger and Schlögl, 2026).

Video supplement. Animations for the "what-if" scenarios (Fig. 10) and the hindcasts (Figs. 11, 12) are available at: https://doi.org/10.6084/m9.figshare.30271795 (Steger, 2025).

Author contributions. SS: conceptualization, data curation, analysis/modelling, validation, visualisation, writing (original draft). RS: conceptualization, data curation (geo-environmental predictors), validation, writing (review and editing). MM: conceptualization, data curation (basins, exposure), writing (review and editing). SL: curation (CERRA data), writing (review and editing). KE: data curation (impact data), writing (review and editing). AC: conceptualization, data curation (CERRA support), writing (review and editing); MS: conceptualization, writing (parts of original draft, review and editing). All authors have read and agreed to the published version of the paper.

Competing interests. At least one of the (co-)authors is a member of the editorial board of *Natural Hazards and Earth System Sciences*. The peer-review process was guided by an independent editor, and the authors also have no other competing interests to declare.

Disclaimer. Publisher's note: Copernicus Publications remains neutral with regard to jurisdictional claims made in the text, published maps, institutional affiliations, or any other geographical representation in this paper. The authors bear the ultimate responsibility for providing appropriate place names. Views expressed in the text are those of the authors and do not necessarily reflect the views of the publisher.

Acknowledgements. We thank Nicola Nocentini and two anonymous reviewers for their valuable feedback.

Financial support. The research leading to these results has received funding from Interreg Alpine Space Program 2021-27 under the project number ASP0100101, "How to adapt to changing weather eXtremes and associated compound and cascading RISKs in the context of Climate Change" (X-RISK-CC).

Review statement. This paper was edited by Mihai Niculita and reviewed by Nicola Nocentini and three anonymous referees.

References

Ahmed, M., Tanyas, H., Huser, R., Dahal, A., Titti, G., Borgatti, L., Francioni, M., and Lombardo, L.: Dynamic rainfall-induced landslide susceptibility: A step towards a unified forecasting system, Int. J. Appl. Earth Obs., 125, 103593, https://doi.org/10.1016/j.jag.2023.103593, 2023.

Alfieri, L., Salamon, P., Pappenberger, F., Wetterhall, F., and Thielen, J.: Operational early warning systems for water-related hazards in Europe, Environ. Sci. Policy, 21, 35–49, https://doi.org/10.1016/j.envsci.2012.01.008, 2012.

Alfieri, L., Libertino, A., Campo, L., Dottori, F., Gabellani, S., Ghizzoni, T., Masoero, A., Rossi, L., Rudari, R., Testa, N., Trasforini, E., Amdihun, A., Ouma, J., Tramblay, Y., Wu, H., and Massabò, M.: Impact-based flood forecasting in the Greater Horn of Africa, Nat. Hazards Earth Syst. Sci., 24, 199–224, https://doi.org/10.5194/nhess-24-199-2024, 2024.

Alvioli, M., Marchesini, I., Reichenbach, P., Rossi, M., Ardizzone, F., Fiorucci, F., and Guzzetti, F.: Automatic delineation of geomorphological slope units with r.slopeunits v1.0 and their optimization for landslide susceptibility modeling, Geosci. Model Dev., 9, 3975–3991, https://doi.org/10.5194/gmd-9-3975-2016, 2016.

Antonetti, G., Gentilucci, M., Aringoli, D., and Pambianchi, G.: Analysis of landslide Susceptibility and Tree Felling Due to an Extreme Event at Mid-Latitudes: Case Study of Storm Vaia, Italy, Land, 11, 1808, https://doi.org/10.3390/land11101808, 2022.

Ardizzone, F., Cardinali, M., Carrara, A., Guzzetti, F., and Reichenbach, P.: Impact of mapping errors on the reliability of landslide hazard maps, Nat. Hazards Earth Syst. Sci., 2, 3–14, https://doi.org/10.5194/nhess-2-3-2002, 2002.

Auflič, M. J., Šinigoj, J., Krivic, M., Podboj, M., Peternel, T., and Komac, M.: Landslide prediction System for rainfall induced landslides in Slovenia (Masprem), Geologija, 59, 259–271, https://doi.org/10.5474/geologija.2016.016, 2016.

Benestad, R., Caron, L.-P., Parding, K., Iturbide, M., Llorente, J. M. G., Mezghani, A., and Doblas-Reyes, F. J.: Using statistical downscaling to assess skill of decadal predictions, Tellus A Dyn. Meteorol. Oceanogr., 71, https://doi.org/10.1080/16000870.2019.1652882, 2019.

BMNT: Richtlinie für den Wildbach- und Lawinenkataster (WLK-RL), BMLFUW-LE.3.3.3/0034-III/5/2017 Fassung: Mai 2018, https://www.bmluk.gv.at/dam/jcr:ad84fd20-46ab-4560-9789-ecb861fbc3b4/Richtlinie%20f%C3%BCr%20den%20Wildbach-%20und%20Lawinenkataster.pdf (last access: 22 January 2026), 2018.

Brenning, A. and Suesse, T.: Aligning Validation with Deployment in Spatial Prediction: Target-Weighted Cross-Validation, arXiv, https://doi.org/10.48550/arXiv.2603.29981, 2026.

Broeckx, J., Vanmaercke, M., Duchateau, R., and Poesen, J.: A data-based landslide susceptibility map of Africa, Earth Sci. Rev., 185, 102–121, https://doi.org/10.1016/j.earscirev.2018.05.002, 2018.

Brunetti, M. T., Peruccacci, S., Rossi, M., Luciani, S., Valigi, D., and Guzzetti, F.: Rainfall thresholds for the possible occurrence of landslides in Italy, Nat. Hazards Earth Syst. Sci., 10, 447–458, https://doi.org/10.5194/nhess-10-447-2010, 2010.

Budimir, M., Šakić Trogrlić, R., Almeida, C., Arestegui, M., Chuquisengo Vásquez, O., Cisneros, A., Cuba Iriarte, M., Dia, A., Lizon, L., Madueño, G., Ndiaye, A., Ordoñez Caldas, M., Rahman, T., RanaTharu, B., Sall, A., Uprety, D., Anderson, C., and McQuistan, C.: Opportunities and challenges for people-centered multi-hazard early warning systems: Perspectives from the Global South, iScience, 28, 112353, https://doi.org/10.1016/j.isci.2025.112353, 2025.

Caleca, F., Confuorto, P., Raspini, F., Segoni, S., Tofani, V., Casagli, N., and Moretti, S.: Shifting from traditional landslide occurrence modeling to scenario estimation with a "glass-box" machine learning, Sci. Total Environ., 950, 175277, https://doi.org/10.1016/j.scitotenv.2024.175277, 2024.

Caleca, F., Lombardo, L., Steger, S., Tanyas, H., Raspini, F., Dahal, A., Nefros, C., Mărgărint, M. C., Drouin, V., Jemec-Auflič, M., Novellino, A., Tonini, M., Loche, M., Casagli, N., and Tofani, V.: Pan-European Landslide Risk Assessment: From Theory to Practice, Rev. Geophys., 63, https://doi.org/10.1029/2023RG000825, 2025.

Casteel, M. A.: Communicating Increased Risk: An Empirical Investigation of the National Weather Service's Impact-Based Warnings, Weather Clim. Soc, 8, https://doi.org/10.1175/WCAS-D-15-0044.1, 2016.

Cavaleri, L., Bajo, M., Barbariol, F., Bastianini, M., Benetazzo, A., Bertotti, L., Chiggiato, J., Davolio, S., Ferrarin, C., Magnusson, L., Papa, A., Pezzutto, P., Pomaro, A., and Umgiesser, G.: The October 29, 2018 storm in Northern Italy – An exceptional event and its modeling, Prog. Oceanogr., 178, 102178, https://doi.org/10.1016/j.pocean.2019.102178, 2019.

Clement, T. P.: Complexities in Hindcasting Models—When Should We Say Enough Is Enough?, Groundwater, 49, 620–629, https://doi.org/10.1111/j.1745-6584.2010.00765.x, 2011.

Collini, E., Palesi, L. A. I., Nesi, P., Pantaleo, G., Nocentini, N., and Rosi, A.: Predicting and Understanding Landslide Events With Explainable AI, IEEE Access, 10, 31175–31189, https://doi.org/10.1109/ACCESS.2022.3158328, 2022.

Conrad, O., Bechtel, B., Bock, M., Dietrich, H., Fischer, E., Gerlitz, L., Wehberg, J., Wichmann, V., and Böhner, J.: System for Automated Geoscientific Analyses (SAGA) v. 2.1.4, Geosci. Model Dev., 8, 1991–2007, https://doi.org/10.5194/gmd-8-1991-2015, 2015.

Corominas, J., van Westen, C., Frattini, P., Cascini, L., Malet, J.-P., Fotopoulou, S., Catani, F., Van Den Eeckhaut, M., Mavrouli, O., Agliardi, F., Pitilakis, K., Winter, M. G., Pastor, M., Ferlisi, S., Tofani, V., Hervás, J., and Smith, J. T.: Recommendations for the quantitative analysis of landslide risk, Bull. Eng. Geol. Environ., https://doi.org/10.1007/s10064-013-0538-8, 2013.

Crespi, A., Enigl, K., Lehner, S., Haslinger, K., and Pittore, M.: Detection and characterization of precipitation extremes and geohydrological hazards over a transboundary Alpine area based on different methods and climate datasets, Nat. Hazards Earth Syst. Sci., 26, 1975–1996, https://doi.org/10.5194/nhess-26-1975-2026, 2026.

Crozier, M. J.: Landslides: causes, consequences & environment, Routledge, London; New York, ISBN 9780415039673, 1989.

Crozier, M. J.: Prediction of rainfall-triggered landslides: a test of the Antecedent Water Status Model, Earth Surf. Process. Landf., 24, 825–833, https://doi.org/10.1002/(SICI)1096-9837(199908)24:9<825::AID-ESP14>3.0.CO;2-M, 1999.

Dai, F. C., Lee, C. F., and Ngai, Y. Y.: Landslide risk assessment and management: an overview, Eng. Geol., 64, 65–87, https://doi.org/10.1016/S0013-7952(01)00093-X, 2002.

D'Amboise, C., Teich, M., Hormes, A., Steger, S., and Berger, F.: Modeling Protective Forests for Gravitational Natural Hazards and How It Relates to Risk-Based Decision Support Tools, https://doi.org/10.5772/intechopen.99510, 2021.

Donnini, M., Marchesini, I., and Zucchini, A.: A new Alpine geo-lithological map (Alpine-Geo-LiM) and global carbon cycle implications, GSA Bulletin, 132, 2004–2022, https://doi.org/10.1130/B35236.1, 2020.

Dornik, A., Drăguţ, L., Oguchi, T., Hayakawa, Y., and Micu, M.: Influence of sampling design on landslide susceptibility modeling in lithologically heterogeneous areas, Sci. Rep., 12, 2106, https://doi.org/10.1038/s41598-022-06257-w, 2022.

Dupire, S., Toe, D., Barré, J.-B., Bourrier, F., and Berger, F.: Harmonized mapping of forests with a protection function against rockfalls over European Alpine countries, App. Geogr., 120, 102221, https://doi.org/10.1016/j.apgeog.2020.102221, 2020.

Farvacque, M., Lopez-Saez, J., Corona, C., Toe, D., Bourrier, F., and Eckert, N.: How is rockfall risk impacted by land-use and land-cover changes? Insights from the French Alps, Glob. Planet. Change, 174, 138–152, https://doi.org/10.1016/j.gloplacha.2019.01.009, 2019.

Fawcett, T.: An introduction to ROC analysis, Pattern Recognit. Lett., 27, 861–874, https://doi.org/10.1016/j.patrec.2005.10.010, 2006.

Fosser, G., Khodayar, S., and Berg, P.: Benefit of convection permitting climate model simulations in the representation of convective precipitation, Clim. Dyn., 44, 45–60, https://doi.org/10.1007/s00382-014-2242-1, 2015.

Fosser, G., Gaetani, M., Kendon, E. J., Adinolfi, M., Ban, N., Belušić, D., Caillaud, C., Careto, J. A. M., Coppola, E., Demory, M.-E., de Vries, H., Dobler, A., Feldmann, H., Goergen, K., Lenderink, G., Pichelli, E., Schär, C., Soares, P. M. M., Somot, S., and Tölle, M. H.: Convection-permitting climate models offer more certain extreme rainfall projections, npj Clim. Atmos. Sci., 7, 51, https://doi.org/10.1038/s41612-024-00600-w, 2024.

Fuchs, S., Röthlisberger, V., Thaler, T., Zischg, A., and Keiler, M.: Natural Hazard Management from a Coevolutionary Perspective: Exposure and Policy Response in the European Alps, Ann. Am. Assoc. Geogr., 107, 382–392, https://doi.org/10.1080/24694452.2016.1235494, 2017.

Gariano, S. L. and Guzzetti, F.: Landslides in a changing climate, Earth Sci. Rev., 162, 227–252, https://doi.org/10.1016/j.earscirev.2016.08.011, 2016.

Giorgi, F., Torma, C., Coppola, E., Ban, N., Schär, C., and Somot, S.: Enhanced summer convective rainfall at Alpine high elevations in response to climate warming, Nature Geosci., 9, 584–589, https://doi.org/10.1038/ngeo2761, 2016.

Giovannini, L., Davolio, S., Zaramella, M., Zardi, D., and Borga, M.: Multi-model convection-resolving simulations of the October 2018 Vaia storm over Northeastern Italy, Atmos. Res., 253, 105455, https://doi.org/10.1016/j.atmosres.2021.105455, 2021.

Godina, R. and Müller, G.: Das Hochwasser in Österreich vom 22. bis 30. Juni 2009, Beschreibung der hydrologischen Situation Abteilung VII/3–Wasserhaushalt (HZB), Bundesministerium für Land-und Forstwirtschaft, Umwelt und Wasserwirtschaft, Vienna, https://www.bmluk.gv.at/dam/jcr:82a5bf7d-85cc-4d55-81e4-1a94d362bee8/Bericht_20Hochwasser_20_20VII3_Juni_202009_20HP_20V1_01[].pdf (last access: 5 August 2026), 2009.

Goetz, J. N., Brenning, A., Petschko, H., and Leopold, P.: Evaluating machine learning and statistical prediction techniques for landslide susceptibility modeling, Comput. Geosci., 81, 1–11, https://doi.org/10.1016/j.cageo.2015.04.007, 2015.

Goodchild, M. F.: Citizens as sensors: the world of volunteered geography, GeoJournal, 69, 211–221, https://doi.org/10.1007/s10708-007-9111-y, 2007.

Greenwell, B. and Boehmke, B.: Variable Importance Plots-An Introduction to the vip Package, The R Journal, 12, 343–366, https://doi.org/10.32614/RJ-2020-013, 2020.

Günther, A., Van Den Eeckhaut, M., Malet, J.-P., Reichenbach, P., and Hervás, J.: Climate-physiographically differentiated Pan-European landslide susceptibility assessment using spatial multi-criteria evaluation and transnational landslide information, Geomorphology, 224, 69–85, https://doi.org/10.1016/j.geomorph.2014.07.011, 2014.

Guo, Z., Tian, B., Zhu, Y., He, J., and Zhang, T.: How do the landslide and non-landslide sampling strategies impact landslide susceptibility assessment? – A catchment-scale case study from China, J. Rock Mech. Geotech. Eng., 16, 877–894, https://doi.org/10.1016/j.jrmge.2023.07.026, 2024.

Guzzetti, F., Reichenbach, P., Ardizzone, F., Cardinali, M., and Galli, M.: Estimating the quality of landslide susceptibility models, Geomorphology, 81, 166–184, https://doi.org/10.1016/j.geomorph.2006.04.007, 2006.

Guzzetti, F., Gariano, S. L., Peruccacci, S., Brunetti, M. T., Marchesini, I., Rossi, M., and Melillo, M.: Geographical landslide early warning systems, Earth Sci. Rev., 200, 102973, https://doi.org/10.1016/j.earscirev.2019.102973, 2020.

Hearn, G. J. and Hart, A. B.: Landslide susceptibility mapping: a practitioner's view, Bull. Eng. Geol. Environ., 78, 5811–5826, https://doi.org/10.1007/s10064-019-01506-1, 2019.

Heiser, M., Hübl, J., and Scheidl, C.: Completeness analyses of the Austrian torrential event catalog, Landslides, 16, 2115–2126, https://doi.org/10.1007/s10346-019-01218-3, 2019.

Heiser, M., Schlögl, M., Spangl, B., Fuchs, S., Rickenmann, D., Zimmermann, M., and Scheidl, C.: Repose time patterns of debris-flow events in alpine catchments, Earth Surf. Process. Landf., 48, 1034–1051, https://doi.org/10.1002/esp.5533, 2023.

Hofstätter, M. and Chimani, B.: Van Bebber's cyclone tracks at 700 hPa in the Eastern Alps for 1961–2002 and their comparison to Circulation Type Classifications, Meteorol. Z., 459–473, https://doi.org/10.1127/0941-2948/2012/0473, 2012.

Hornich, R. and Adelwöhrer, R.: Landslides in Styria in 2009/Hangrutschungsereignisse 2009 in der Steiermark, Geomech. Tunn., 3, 455–461, https://doi.org/10.1002/geot.201000042, 2010.

Horton, P., Jaboyedoff, M., Rudaz, B., and Zimmermann, M.: Flow-R, a model for susceptibility mapping of debris flows and other gravitational hazards at a regional scale, Nat. Hazards Earth Syst. Sci., 13, 869–885, https://doi.org/10.5194/nhess-13-869-2013, 2013.

Iadanza, C., Trigila, A., Starace, P., Dragoni, A., Biondo, T., and Roccisano, M.: IdroGEO: A Collaborative Web Mapping Application Based on REST API Services and Open Data on Landslides and Floods in Italy, ISPRS Int. J. Geo-Inf., 10, 89, https://doi.org/10.3390/ijgi10020089, 2021.

Kaitna, R., Schlögl, M., Becsi, B., Rieder, H., and Formayer, H.: Climate induced increase in frequency and area affected by critical rainfall conditions triggering debris flows in Austria, Commun. Earth Environ., 6, 793, https://doi.org/10.1038/s43247-025-02760-w, 2025.

Kaltenberger, R., Schaffhauser, A., and Staudinger, M.: "What the weather will do" – results of a survey on impact-oriented and impact-based warnings in European NMHSs, Adv. Sci. Res., 17, 29–38, https://doi.org/10.5194/asr-17-29-2020, 2020.

Keiler, M. and Fuchs, S.: Vulnerability and Exposure to Geomorphic Hazards: Some Insights from the European Alps, in: Geomorphology and Society, edited by: Meadows, M. E. and Lin, J.-C., Springer Japan, Tokyo, 165–180, https://doi.org/10.1007/978-4-431-56000-5_10, 2016.

Knevels, R., Petschko, H., Proske, H., Leopold, P., Maraun, D., and Brenning, A.: Event-Based Landslide Modeling in the Styrian Basin, Austria: Accounting for Time-Varying Rainfall and Land Cover, Geosciences, 10, 217, https://doi.org/10.3390/geosciences10060217, 2020.

Krøgli, I. K., Devoli, G., Colleuille, H., Boje, S., Sund, M., and Engen, I. K.: The Norwegian forecasting and warning service for rainfall- and snowmelt-induced landslides, Nat. Hazards Earth Syst. Sci., 18, 1427–1450, https://doi.org/10.5194/nhess-18-1427-2018, 2018.

Lazoglou, G., Economou, T., Anagnostopoulou, C., Zittis, G., Tzyrkalli, A., Georgiades, P., and Lelieveld, J.: Multivariate adjustment of drizzle bias using machine learning in European climate projections, Geosci. Model Dev., 17, 4689–4703, https://doi.org/10.5194/gmd-17-4689-2024, 2024.

Lima, P., Steger, S., and Glade, T.: Counteracting flawed landslide data in statistically based landslide susceptibility modelling for very large areas: a national-scale assessment for Austria, Landslides, 18, 3531–3546, https://doi.org/10.1007/s10346-021-01693-7, 2021.

Lima, P., Steger, S., Glade, T., and Murillo-García, F. G.: Literature review and bibliometric analysis on data-driven assessment of landslide susceptibility, J. Mt. Sci., 19, 1670–1698, https://doi.org/10.1007/s11629-021-7254-9, 2022.

Lima, P., Steger, S., Glade, T., and Mergili, M.: Conventional data-driven landslide susceptibility models may only tell us half of the story: Potential underestimation of landslide impact areas depending on the modeling design, Geomorphology, 430, 108638, https://doi.org/10.1016/j.geomorph.2023.108638, 2023.

Lin, Q., Steger, S., Pittore, M., Zhang, Y., Zhang, J., Zhou, L., Wang, L., Wang, Y., and Jiang, T.: Contrasting Population Projections to Induce Divergent Estimates of Landslides Exposure Under Climate Change, Earth's Future, 11, https://doi.org/10.1029/2023EF003741, 2023.

Loche, M., Alvioli, M., Marchesini, I., Bakka, H., and Lombardo, L.: Landslide susceptibility maps of Italy: Lesson learnt from dealing with multiple landslide types and the uneven spatial distribution of the national inventory, Earth Sci. Rev., 232, 104125, https://doi.org/10.1016/j.earscirev.2022.104125, 2022.

Lombardo, L., Opitz, T., and Huser, R.: Point process-based modeling of multiple debris flow landslides using INLA: an application to the 2009 Messina disaster, Stoch. Environ. Res. Risk Assess., 32, 2179–2198, https://doi.org/10.1007/s00477-018-1518-0, 2018.

Lombardo, L., Opitz, T., Ardizzone, F., Guzzetti, F., and Huser, R.: Space-time landslide predictive modelling, Earth Sci. Rev., 209, 103318, https://doi.org/10.1016/j.earscirev.2020.103318, 2020.

Luna, L. V. and Korup, O.: Seasonal Landslide Activity Lags Annual Precipitation Pattern in the Pacific Northwest, Geophys. Res. Lett., 49, https://doi.org/10.1029/2022GL098506, 2022.

Luna, L. V., Woodard, J. B., Bytheway, J. L., Belair, G. M., and Mirus, B. B.: Constraining landslide frequency across the United States to inform county-level risk reduction, Nat. Hazards Earth Syst. Sci., 25, 3279–3307, https://doi.org/10.5194/nhess-25-3279-2025, 2025.

Maier, H. R., Rosa Taghikhah, F., Nabavi, E., Razavi, S., Gupta, H., Wu, W., Radford, D. A. G., and Huang, J.: How much X is in XAI: Responsible use of "Explainable" artificial intelligence in hydrology and water resources, J. Hydrol. X, 25, 100185, https://doi.org/10.1016/j.hydroa.2024.100185, 2024.

Malinowski, R., Lewiński, S., Rybicki, M., Gromny, E., Jenerowicz, M., Krupiński, M., Nowakowski, A., Wojtkowski, C., Krätzschmar, E., and Schauer, P.: Automated Production of a Land Cover/Use Map of Europe Based on Sentinel-2 Imagery, Remote Sens., 12, 3523, https://doi.org/10.3390/rs12213523, 2020.

Maraun, D., Knevels, R., Mishra, A. N., Truhetz, H., Bevacqua, E., Proske, H., Zappa, G., Brenning, A., Petschko, H., Schaffer, A., Leopold, P., and Puxley, B. L.: A severe landslide event in the Alpine foreland under possible future climate and land-use changes, Commun. Earth Environ., 3, 1–11, https://doi.org/10.1038/s43247-022-00408-7, 2022.

Marchesini, I., Althuwaynee, O., Santangelo, M., Alvioli, M., Cardinali, M., Mergili, M., Reichenbach, P., Peruccacci, S., Balducci, V., Agostino, I., Esposito, R., and Rossi, M.: National-scale assessment of railways exposure to rapid flow-like landslides, Eng. Geol., 332, 107474, https://doi.org/10.1016/j.enggeo.2024.107474, 2024.

Marra, F., Nikolopoulos, E. I., Creutin, J. D., and Borga, M.: Space–time organization of debris flows-triggering rainfall and its effect on the identification of the rainfall threshold relationship, J. Hydrol., 541, 246–255, https://doi.org/10.1016/j.jhydrol.2015.10.010, 2016.

Marra, G. and Wood, S. N.: Practical variable selection for generalized additive models, Comput. Stat. Data Anal., 55, 2372–2387, https://doi.org/10.1016/j.csda.2011.02.004, 2011.

Menegatto, M., Freschi, G., Bulfon, M., and Zamperini, A.: Collectively Remembering Environmental Disasters: The Vaia Storm as a Case Study, Sustainability, 16, 8418, https://doi.org/10.3390/su16198418, 2024.

Ménégoz, M., Valla, E., Jourdain, N. C., Blanchet, J., Beaumet, J., Wilhelm, B., Gallée, H., Fettweis, X., Morin, S., and Anquetin, S.: Contrasting seasonal changes in total and intense precipitation in the European Alps from 1903 to 2010, Hydrol. Earth Syst. Sci., 24, 5355–5377, https://doi.org/10.5194/hess-24-5355-2020, 2020.

Menk, J., Berger, F., Moos, C., and Dorren, L.: Towards an improved rapid assessment tool for rockfall protection forests using field-mapped deposited rocks, Geomorphology, 422, 108520, https://doi.org/10.1016/j.geomorph.2022.108520, 2023.

Mergili, M., Krenn, J., and Chu, H.-J.: r.randomwalk v1, a multi-functional conceptual tool for mass movement routing, Geosci. Model Dev., 8, 4027–4043, https://doi.org/10.5194/gmd-8-4027-2015, 2015.

Mergili, M., Schwarz, L., and Kociu, A.: Combining release and runout in statistical landslide susceptibility modeling, Landslides, 16, 2151–2165, https://doi.org/10.1007/s10346-019-01222-7, 2019.

Merz, B., Kuhlicke, C., Kunz, M., Pittore, M., Babeyko, A., Bresch, D. N., Domeisen, D. I. V., Feser, F., Koszalka, I., Kreibich, H., Pantillon, F., Parolai, S., Pinto, J. G., Punge, H. J., Rivalta, E., Schröter, K., Strehlow, K., Weisse, R., and Wurpts, A.: Impact Forecasting to Support Emergency Management of Natural Hazards, Rev. Geophys., 58, https://doi.org/10.1029/2020RG000704, 2020.

Metz, C. E.: Basic principles of ROC analysis, Semin. Nucl. Med., 8, 283–298, https://doi.org/10.1016/S0001-2998(78)80014-2, 1978.

Mirus, B. B., Becker, R. E., Baum, R. L., and Smith, J. B.: Integrating real-time subsurface hydrologic monitoring with empirical rainfall thresholds to improve landslide early warning, Landslides, 15, 1909–1919, https://doi.org/10.1007/s10346-018-0995-z, 2018.

Mishra, A. N., Maraun, D., Knevels, R., Truhetz, H., Brenning, A., and Proske, H.: Climate change amplified the 2009 extreme landslide event in Austria, Clim. Change, 176, 124, https://doi.org/10.1007/s10584-023-03593-2, 2023.

Molnar, C.: Interpretable Machine Learning. A Guide for Making Black Box Models Explainable, 320 pp., https://christophm.github.io/interpretable-ml-book (last access: 22 January 2026), 2025.

Mondini, A. C., Guzzetti, F., Melillo, M., and Pievatolo, A.: Short to long term space-time prediction of rain-induced landslides under uncertainty, Sci. Total Environ., 984, 179453, https://doi.org/10.1016/j.scitotenv.2025.179453, 2025.

Moreno, M., Lombardo, L., Crespi, A., Zellner, P. J., Mair, V., Pittore, M., van Westen, C., and Steger, S.: Space-time data-driven modeling of precipitation-induced shallow landslides in South Tyrol, Italy, Sci. Total Environ., 912, 169166, https://doi.org/10.1016/j.scitotenv.2023.169166, 2024.

Moreno, M., Lombardo, L., Steger, S., de Vugt, L., Zieher, T., Crespi, A., Marra, F., van Westen, C., and Opitz, T.: Functional Regression for Space-Time Prediction of Precipitation-Induced Shallow Landslides in South Tyrol, Italy, J. Geophys. Res.-Earth Surf., 130, https://doi.org/10.1029/2024JF008219, 2025.

Najafi, H., Shrestha, P. K., Rakovec, O., Apel, H., Vorogushyn, S., Kumar, R., Thober, S., Merz, B., and Samaniego, L.: High-resolution impact-based early warning system for riverine flooding, Nat. Commun., 15, 3726, https://doi.org/10.1038/s41467-024-48065-y, 2024.

Neteler, M., Bowman, M. H., Landa, M., and Metz, M.: GRASS GIS: A multi-purpose open source GIS, Environ. Modell. Softw., 31, 124–130, 2012.

Nocentini, N., Rosi, A., Segoni, S., and Fanti, R.: Towards landslide space-time forecasting through machine learning: the influence of rainfall parameters and model setting, Front. Earth Sci., 11, https://doi.org/10.3389/feart.2023.1152130, 2023.

Nocentini, N., Rosi, A., Piciullo, L., Liu, Z., Segoni, S., and Fanti, R.: Regional-scale spatiotemporal landslide probability assessment through machine learning and potential applications for operational warning systems: a case study in Kvam (Norway), Landslides, 21, 2369–2387, https://doi.org/10.1007/s10346-024-02287-9, 2024.

Oh, J. and Bartos, M.: Flood early warning system with data assimilation enables site-level forecasting of bridge impacts, npj Nat. Hazards, 2, 64, https://doi.org/10.1038/s44304-025-00116-0, 2025.

Ozturk, U., Saito, H., Matsushi, Y., Crisologo, I., and Schwanghart, W.: Can global rainfall estimates (satellite and reanalysis) aid landslide hindcasting?, Landslides, 18, 3119–3133, https://doi.org/10.1007/s10346-021-01689-3, 2021.

Ozturk, U., Bozzolan, E., Holcombe, E. A., Shukla, R., Pianosi, F., and Wagener, T.: How climate change and unplanned urban sprawl bring more landslides, Nature, 608, 262–265, https://doi.org/10.1038/d41586-022-02141-9, 2022.

Pacheco Quevedo, R., Velastegui-Montoya, A., Montalván-Burbano, N., Morante-Carballo, F., Korup, O., and Daleles Rennó, C.: Land use and land cover as a conditioning factor in landslide susceptibility: a literature review, Landslides, 20, 967–982, https://doi.org/10.1007/s10346-022-02020-4, 2023.

Pedersen, E. J., Miller, D. L., Simpson, G. L., and Ross, N.: Hierarchical generalized additive models in ecology: an introduction with mgcv, PeerJ, 7, https://doi.org/10.7717/peerj.6876, 2019.

Peres, D. J. and Cancelliere, A.: Comparing methods for determining landslide early warning thresholds: potential use of non-triggering rainfall for locations with scarce landslide data availability, Landslides, 18, 3135–3147, https://doi.org/10.1007/s10346-021-01704-7, 2021.

Petschko, H., Brenning, A., Bell, R., Goetz, J., and Glade, T.: Assessing the quality of landslide susceptibility maps – case study Lower Austria, Nat. Hazards Earth Syst. Sci., 14, 95–118, https://doi.org/10.5194/nhess-14-95-2014, 2014.

Piciullo, L., Calvello, M., and Cepeda, J. M.: Territorial early warning systems for rainfall-induced landslides, Earth Sci. Rev., 179, 228–247, https://doi.org/10.1016/j.earscirev.2018.02.013, 2018.

Pisano, L., Zumpano, V., Malek, Ž., Rosskopf, C. M., and Parise, M.: Variations in the susceptibility to landslides, as a consequence of land cover changes: A look to the past, and another towards the future, Sci. Total Environ., 601–602, 1147–1159, https://doi.org/10.1016/j.scitotenv.2017.05.231, 2017.

Pittore, M., Wieland, M., and Fleming, K.: Perspectives on global dynamic exposure modelling for geo-risk assessment, Nat. Hazards, 86, 7–30, https://doi.org/10.1007/s11069-016-2437-3, 2017.

Potter, S., Harrison, S., and Kreft, P.: The Benefits and Challenges of Implementing Impact-Based Severe Weather Warning Systems: Perspectives of Weather, Flood, and Emergency Management Personnel, Weather Clim. Soc., 13, 303–314, https://doi.org/10.1175/WCAS-D-20-0110.1, 2021.

Rabby, Y. W., Li, Y., and Hilafu, H.: An objective absence data sampling method for landslide susceptibility mapping, Sci. Rep., 13, 1740, https://doi.org/10.1038/s41598-023-28991-5, 2023.

Reichenbach, P., Rossi, M., Malamud, B. D., Mihir, M., and Guzzetti, F.: A review of statistically-based landslide susceptibility models, Earth Sci. Rev., 180, 60–91, https://doi.org/10.1016/j.earscirev.2018.03.001, 2018.

Reichstein, M., Benson, V., Blunk, J., Camps-Valls, G., Creutzig, F., Fearnley, C. J., Han, B., Kornhuber, K., Rahaman, N., Schölkopf, B., Tárraga, J. M., Vinuesa, R., Dall, K., Denzler, J., Frank, D., Martini, G., Nganga, N., Maddix, D. C., and Weldemariam, K.: Early warning of complex climate risk with integrated artificial intelligence, Nat. Commun., 16, 2564, https://doi.org/10.1038/s41467-025-57640-w, 2025.

Renwick, W. H.: Equilibrium, disequilibrium, and nonequilibrium landforms in the landscape, Geomorphology, 5, 265–276, https://doi.org/10.1016/0169-555X(92)90008-C, 1992.

Ridal, M., Bazile, E., Le Moigne, P., Randriamampianina, R., Schimanke, S., Andrae, U., Berggren, L., Brousseau, P., Dahlgren, P., Edvinsson, L., El-Said, A., Glinton, M., Hagelin, S., Hopsch, S., Isaksson, L., Medeiros, P., Olsson, E., Unden, P., and

Wang, Z. Q.: CERRA, the Copernicus European Regional Reanalysis system, Q. J. R. Meteorol. Soc., 150, 3385–3411, https://doi.org/10.1002/qj.4764, 2024.

Rosi, A., Segoni, S., Canavesi, V., Monni, A., Gallucci, A., and Casagli, N.: Definition of 3D rainfall thresholds to increase operative landslide early warning system performances, Landslides, 18, 1045–1057, https://doi.org/10.1007/s10346-020-01523-2, 2021.

Schär, C., Davies, T. D., Frei, C., Wanner, H., Widmann, M., Wild, M., and Davies, H. C.: Current alpine climate, Views from the Alps: Regional perspectives on climate change, 21, 63, ISBN 0-262-03252-X, 1998.

Schisterman, E. F., Perkins, N. J., Liu, A., and Bondell, H.: Optimal cut-point and its corresponding Youden Index to discriminate individuals using pooled blood samples, Epidemiology, 73–81, https://doi.org/10.1097/01.ede.0000147512.81966.ba, 2005.

Schlögl, M., Richter, G., Avian, M., Thaler, T., Heiss, G., Lenz, G., and Fuchs, S.: On the nexus between landslide susceptibility and transport infrastructure – an agent-based approach, Nat. Hazards Earth Syst. Sci., 19, 201–219, https://doi.org/10.5194/nhess-19-201-2019, 2019.

Schlögl, M., Fuchs, S., Scheidl, C., and Heiser, M.: Trends in torrential flooding in the Austrian Alps: A combination of climate change, exposure dynamics, and mitigation measures, Clim. Risk Manag., 32, 100294, https://doi.org/10.1016/j.crm.2021.100294, 2021.

Schlögl, M., Graser, A., Spiekermann, R., Lampert, J., and Steger, S.: Brief communication: Visualizing uncertainties in landslide susceptibility modelling using bivariate mapping, Nat. Hazards Earth Syst. Sci., 25, 1425–1437, https://doi.org/10.5194/nhess-25-1425-2025, 2025a.

Schlögl, M., Spiekermann, R., and Steger, S.: Towards a holistic assessment of landslide susceptibility models: insights from the Central Eastern Alps, Environ. Earth Sci., 84, 113, https://doi.org/10.1007/s12665-024-12041-y, 2025b.

Schmaltz, E. M., Van Beek, L. P. H., Bogaard, T. A., Kraushaar, S., Steger, S., and Glade, T.: Strategies to improve the explanatory power of a dynamic slope stability model by enhancing land cover parameterisation and model complexity, Earth Surf. Process. Landf., 44, 1259–1273, https://doi.org/10.1002/esp.4570, 2019.

Schmid, T., Portmann, R., Villiger, L., Schröer, K., and Bresch, D. N.: An open-source radar-based hail damage model for buildings and cars, Nat. Hazards Earth Syst. Sci., 24, 847–872, https://doi.org/10.5194/nhess-24-847-2024, 2024.

Schratz, P., Becker, M., Lang, M., and Brenning, A.: Mlr3spatiotempcv: Spatiotemporal resampling methods for machine learning in R, J. Stat. Softw., 111, 1–36, https://doi.org/10.18637/jss.v111.i07, 2024.

Sebald, J., Senf, C., Heiser, M., Scheidl, C., Pflugmacher, D., and Seidl, R.: The effects of forest cover and disturbance on torrential hazards: large-scale evidence from the Eastern Alps, Environ. Res. Lett., 14, 114032, https://doi.org/10.1088/1748-9326/ab4937, 2019.

Segoni, S., Piciullo, L., and Gariano, S. L.: A review of the recent literature on rainfall thresholds for landslide occurrence, Landslides, 15, 1483–1501, https://doi.org/10.1007/s10346-018-0966-4, 2018.

Segoni, S., Nocentini, N., Barbadori, F., Medici, C., Gatto, A., Rosi, A., and Casagli, N.: A novel prototype national-scale landslide nowcasting system for Italy combining rainfall thresholds and risk indicators, Landslides, 22, 1341–1366, https://doi.org/10.1007/s10346-024-02452-0, 2025.

Sidle, R. C. and Ochiai, H.: Natural Factors Influencing Landslides, in: Landslides: Processes, Prediction, and Land Use, American Geophysical Union (AGU), 41–119, https://doi.org/10.1002/9781118665954.ch3, 2006.

Simpson, G. L.: Gratia: An R package for exploring generalized additive models, JOSS, 9, 6962, https://doi.org/10.21105/joss.06962, 2024.

Sivle, A. D., Agersten, S., Schmid, F., and Simon, A.: Use and perception of weather forecast information across Europe, Meteorol. Appl., 29, https://doi.org/10.1002/met.2053, 2022.

Smith, H. G., Neverman, A. J., Betts, H., and Spiekermann, R.: The influence of spatial patterns in rainfall on shallow landslides, Geomorphology, 437, 108795, https://doi.org/10.1016/j.geomorph.2023.108795, 2023.

Sonny: Open LiDAR Digital Terrain Models of Europe; v18, available at: https://sonny.4lima.de (last access: 10 December 2025), 2023.

Stähli, M., Sättele, M., Huggel, C., McArdell, B. W., Lehmann, P., Van Herwijnen, A., Berne, A., Schleiss, M., Ferrari, A., Kos, A., Or, D., and Springman, S. M.: Monitoring and prediction in early warning systems for rapid mass movements, Nat. Hazards Earth Syst. Sci., 15, 905–917, https://doi.org/10.5194/nhess-15-905-2015, 2015.

Stanley, T. A., Kirschbaum, D. B., Benz, G., Emberson, R. A., Amatya, P. M., Medwedeff, W., and Clark, M. K.: Data-Driven Landslide Nowcasting at the Global Scale, Front. Earth Sci., 9, https://doi.org/10.3389/feart.2021.640043, 2021.

Steen, V. A., Tingley, M. W., Paton, P. W. C., and Elphick, C. S.: Spatial thinning and class balancing: Key choices lead to variation in the performance of species distribution models with citizen science data, Methods Ecol. Evol., 12, 216–226, https://doi.org/10.1111/2041-210X.13525, 2021.

Steger, S.: Supplement “Dynamic spatial modelling of mass movement impacts for large areas: A data-driven framework for impact-based early warning”, figshare [video], https://doi.org/10.6084/m9.figshare.30271795.v2, 2025.

Steger, S. and Glade, T.: The Challenge of “Trivial Areas” in Statistical Landslide Susceptibility Modelling, in: Advancing Culture of Living with Landslides, edited by: Mikos, M., Tiwari, B., Yin, Y., and Sassa, K., Springer International Publishing, Cham, 803–808, https://doi.org/10.1007/978-3-319-53498-5_92, 2017.

Steger, S. and Schlögl, M.: Supplementary code and data to “Dynamic spatial modelling of mass movement impacts for large areas: A data-driven framework for impact-based early warning”, Version v1.0, Zenodo [code], https://doi.org/10.5281/zenodo.21645145, 2026.

Steger, S., Brenning, A., Bell, R., Petschko, H., and Glade, T.: Exploring discrepancies between quantitative validation results and the geomorphic plausibility of statistical landslide susceptibility maps, Geomorphology, 262, 8–23, https://doi.org/10.1016/j.geomorph.2016.03.015, 2016a.

Steger, S., Brenning, A., Bell, R., and Glade, T.: The propagation of inventory-based positional errors into statistical landslide susceptibility models, Nat. Hazards Earth Syst. Sci., 16, 2729–2745, https://doi.org/10.5194/nhess-16-2729-2016, 2016b.

Steger, S., Mair, V., Kofler, C., Pittore, M., Zebisch, M., and Schneiderbauer, S.: Correlation does not imply geomorphic causation in data-driven landslide susceptibility modelling – Benefits of exploring landslide data collection effects, Sci. Total Environ., 776, 145935, https://doi.org/10.1016/j.scitotenv.2021.145935, 2021.

Steger, S., Moreno, M., Crespi, A., Zellner, P. J., Gariano, S. L., Brunetti, M. T., Melillo, M., Peruccacci, S., Marra, F., Kohrs, R., Goetz, J., Mair, V., and Pittore, M.: Deciphering seasonal effects of triggering and preparatory precipitation for improved shallow landslide prediction using generalized additive mixed models, Nat. Hazards Earth Syst. Sci., 23, 1483–1506, https://doi.org/10.5194/nhess-23-1483-2023, 2023.

Steger, S., Moreno, M., Crespi, A., Luigi Gariano, S., Teresa Brunetti, M., Melillo, M., Peruccacci, S., Marra, F., de Vugt, L., Zieher, T., Rutzinger, M., Mair, V., and Pittore, M.: Adopting the margin of stability for space–time landslide prediction – A data-driven approach for generating spatial dynamic thresholds, Geosci. Front., 15, 101822, https://doi.org/10.1016/j.gsf.2024.101822, 2024.

Sun, J., Xue, M., Wilson, J. W., Zawadzki, I., Ballard, S. P., Onvlee-Hooimeyer, J., Joe, P., Barker, D. M., Li, P.-W., Golding, B., Xu, M., and Pinto, J.: Use of NWP for Nowcasting Convective Precipitation: Recent Progress and Challenges, Bull. Am. Meteorol. Soc., 95, https://doi.org/10.1175/BAMS-D-11-00263.1, 2014.

Themessl, M., Enigl, K., Reisenhofer, S., Köberl, J., Kortschak, D., Reichel, S., Ostermann, M., Kienberger, S., Tiede, D., Bresch, D. N., Röösli, T., Lehner, D., Schubert, C., Pichler, A., Leitner, M., and Balas, M.: Collection, Standardization and Attribution of Robust Disaster Event Information – A Demonstrator of a National Event-Based Loss and Damage Database in Austria, Geosciences, 12, 283, https://doi.org/10.3390/geosciences12080283, 2022.

Tiranti, D. and Ronchi, C.: Climate Change Impacts on Shallow Landslide Events and on the Performance of the Regional Shallow Landslide Early Warning System of Piemonte (Northwestern Italy), GeoHazards, 4, 475–496, https://doi.org/10.3390/geohazards4040027, 2023.

Trigila, A., Iadanza, C., and Spizzichino, D.: Quality assessment of the Italian Landslide Inventory using GIS processing, Landslides, 7, 455–470, https://doi.org/10.1007/s10346-010-0213-0, 2010.

Uccellini, L. W. and Hoeve, J. E. T.: Evolving the National Weather Service to Build a Weather-Ready Nation: Connecting Observations, Forecasts, and Warnings to Decision-Makers through Impact-Based Decision Support Services, Bull. Am. Meteorol. Soc., 100, https://doi.org/10.1175/BAMS-D-18-0159.1, 2019.

van Natijne, A. L., Bogaard, T. A., Zieher, T., Pfeiffer, J., and Lindenbergh, R. C.: Machine-learning-based nowcasting of the Vögelsberg deep-seated landslide: why predicting slow deformation is not so easy, Nat. Hazards Earth Syst. Sci., 23, 3723–3745, https://doi.org/10.5194/nhess-23-3723-2023, 2023.

van Westen, C. J., Castellanos, E., and Kuriakose, S. L.: Spatial data for landslide susceptibility, hazard, and vulnerability assessment: An overview, Eng. Geol., 102, 112–131, https://doi.org/10.1016/j.enggeo.2008.03.010, 2008.

Vinuesa, R. and Sirmacek, B.: Interpretable deep-learning models to help achieve the Sustainable Development Goals, Nat. Mach. Intell., 3, 926–926, https://doi.org/10.1038/s42256-021-00414-y, 2021.

Wang, Z., Goetz, J., and Brenning, A.: Transfer learning for landslide susceptibility modeling using domain adaptation and case-based reasoning, Geosci. Model Dev., 15, 8765–8784, https://doi.org/10.5194/gmd-15-8765-2022, 2022.

Weyrich, P., Scolobig, A., Bresch, D. N., and Patt, A.: Effects of Impact-Based Warnings and Behavioral Recommendations for Extreme Weather Events, Weather Clim. Soc., 10, 781–796, https://doi.org/10.1175/WCAS-D-18-0038.1, 2018.

Weyrich, P., Scolobig, A., Walther, F., and Patt, A.: Responses to severe weather warnings and affective decision-making, Nat. Hazards Earth Syst. Sci., 20, 2811–2821, https://doi.org/10.5194/nhess-20-2811-2020, 2020.

Wichmann, V.: The Gravitational Process Path (GPP) model (v1.0) – a GIS-based simulation framework for gravitational processes, Geosci. Model Dev., 10, 3309–3327, https://doi.org/10.5194/gmd-10-3309-2017, 2017.

Wicki, A., Lehmann, P., Hauck, C., Seneviratne, S. I., Waldner, P., and Stähli, M.: Assessing the potential of soil moisture measurements for regional landslide early warning, Landslides, 17, 1881–1896, https://doi.org/10.1007/s10346-020-01400-y, 2020.

WMO: World Meteorological Organization: guidelines on multi-hazard impact-based forecast and warning services, WMO Doc., 1150, ISBN 978-92-63-11150-0, 2015.

Wood, S. N.: Generalized Additive Models: An Introduction with R, 2nd edn., Chapman and Hall/CRC, New York, 496 pp., https://doi.org/10.1201/9781315370279, 2017.

Wood, S. N., Goude, Y., and Shaw, S.: Generalized Additive Models for Large Data Sets, J. R. Stat. Soc. Ser. C. Appl. Stat., 64, 139–155, https://doi.org/10.1111/rssc.12068, 2015.

Woodard, J. B., Mirus, B. B., Wood, N. J., Allstadt, K. E., Leshchinsky, B. A., and Crawford, M. M.: Slope Unit Maker (SUMak): an efficient and parameter-free algorithm for delineating slope units to improve landslide modeling, Nat. Hazards Earth Syst. Sci., 24, 1–12, https://doi.org/10.5194/nhess-24-1-2024, 2024.

Zhou, Q., Zhang, Y., Chang, K., and Brovelli, M. A.: Assessing OSM building completeness for almost 13,000 cities globally, Int. J. Digit. Earth, 15, 2400–2421, https://doi.org/10.1080/17538947.2022.2159550, 2022.

Zhu, A.-X., Miao, Y., Liu, J., Bai, S., Zeng, C., Ma, T., and Hong, H.: A similarity-based approach to sampling absence data for landslide susceptibility mapping using data-driven methods, CATENA, 183, 104188, https://doi.org/10.1016/j.catena.2019.104188, 2019.

Zuur, A., Ieno, E. N., Walker, N., Saveliev, A. A., and Smith, G. M.: Mixed Effects Models and Extensions in Ecology with R, Springer, New York, NY, 574 pp., ISBN 9780387874586, 2009.